Development of Antibacterial Biomaterials to Tackle Surface-Associated Infections

A Thesis

Submitted in partial fulfillment for the degree of

Master of Science

as a part of

Integrated Ph.D Programme (Chemical Sciences)

By

Mr. Sreyan Ghosh

New Chemistry Unit

Jawaharlal Nehru Centre for Advanced Scientific Research

(A Deemed University)

Bangalore - 560064 (INDIA)

APRIL-2018

Dedicated to My Family and
Prof. Jayanta Haldar

Declaration

I hereby declare that the matter embodied in the thesis entitled "Development of Antibacterial Biomaterials to Tackle Surface-Associated Infections" is the result of the investigations carried out by me at the New Chemistry Unit, Jawaharlal Nehru Centre for Advanced Scientific Research, Bangalore, India under the supervision of Prof. Jayanta Haldar and that it has not been submitted elsewhere for the award of any degree or diploma.

In keeping with the general practice in reporting the scientific observations, due acknowledgement has been made whenever the work described is based on the findings of other investigators. Any omission that might have occurred due to oversight or error in judgement is regretted.

Sreyan Ghosh

Mr. Sreyan Ghosh

(Integrated PhD student)

Certificate

I hereby certify that the matter embodied in the thesis entitled "Development of Antibacterial Biomaterials to Tackle Surface-Associated Infections" is the result of the investigations carried out by Mr. Sreyan Ghosh at the New Chemistry Unit, Jawaharlal Nehru Centre for Advanced Scientific Research, Bangalore, India under my supervision and that it has not been submitted elsewhere for the award of any degree or diploma.

Jayanta Haldar

Prof. Jayanta Haldar

Acknowledgements

It is a lovely feeling to be loved like a child yet to be treated as a grown up. Baba and Ma, have always nurtured me with love and compassion, imbibing all seeds of humane traits in me. I owe them everything that I have achieved and will be achieving with time. My brother, a constant friend in my ups and downs and my grandparents, who never stopped indulging me with love; without these people, my life would not be this beautiful. In this occasion, I fondly remember my grandfather who had been my best companion and guide during my childhood days.

Coming to JNCASR was like a dream come true for me. But the man who pushed me to dream bigger is my supervisor Prof. Jayanta Haldar. He has always stood by me like a parent figure, criticizing me at the same time holding hands in my downs. His philosophy of cultivating science amazes me and encourages to do something better, every single day.

I consider myself fortunate to be in the same campus with Prof. C. N. R. Rao as his words of constant encouragement and his passion to know more have moved me every time I have attended his lectures.

I would like to thank Prof. H. Ila, Dr. Sridhar Rajaram, Prof. Subi J. George, Prof. M. Eswarmoorthy, Prof. T. Govindaraju, Dr. Ranjani Viswanatha, Prof. Sebastian C. Peter, Prof. Tapas K. Maji, , Dr. Kanishka Biswas, Dr. Sarit S. Agasti, Prof. A. Sundaresan, Prof. Chandrabhas Narayana, Dr. Meher K. Prakash for the courses they taught which helped me to explore more beyond books.

I would like to acknowledge my teachers of Visva Bharati Dept. of Chemistry, Bidhanda, Motinda, Pranabda and Alakanandada who guided me all throughout my college days with their ideas and vision.

My lab mates, cheers to them as they have maintained a homely ambience inside the lab. I extend my gratitude to the alumni members Jiaul, Venky, CD, Diwakara. I would like to acknowledge Saibal Singh, a visiting student for helping me in various chemical reactions.

I would love to thank my classmates Satyajit, Manaswee, Madhulika, Santu, Niloy, Janaky and other friends and seniors for making my JNC life bright and eventful.

I would love to express my sincere thanks to all the academic, administrative, technical, security, library, complab and Dhanwantri people for making life in JNC peaceful and easy.

Preface

Development of antimicrobial surfaces to tackle bacterial infections is of great importance due to the increasing prevalence of antibiotic resistant bacterial strains and healthcare associated infections. Effective antimicrobial surfaces can be based on an anti-adhesive principle that prevents bacteria to adhere, or on bactericidal strategies, i.e. killing organisms either before or after contact is made with the surface. Biocide releasing mechanisms kill pathogens in surroundings by leaching of antimicrobials. Contact killing-based coating can also impart antibacterial properties to different surfaces. But surfaces suffer from dead cell accumulation resulting in spoiling of the surfaces. Biofouling is relevant in a wide range of applications, including but not limited to surgical equipment and protective apparels in hospitals, medical implants, biosensors, textiles, food packaging and food storage, water purification systems, and marine and industrial equipments. Surfaces that resist the nonspecific adsorption of protein and microbes are also vital in catheters, prosthetic devices, and contact lenses. Surfaces have also been developed based on 'kill-release' strategy. These first kill bacteria and then release the dead bacterial cells. In this thesis, we have described the development of various antimicrobial materials to tackle surface associated infections. In chapter 2, we have developed benzophenone based quaternary molecules with both non-degradable and degradable side chains and their solution-phase activity has also been described. They are coated on cotton textile. The antibacterial efficacies of coated cottons are described. The coated cottons showed remarkable activity against Gram-positive pathogens. On degradation of the coating based on the degradable molecules **6** (ester) and **7** (amide), antifouling property was achieved by the surface. Chapter 3 deals with the development of dual-action polymer nanocomposite which showed high activity against Gram-negative bacteria. The most potent nanocomposite **QAm_1-Ag_1** was loaded on hydroxyapatite. The activity and toxicity towards human erythrocytes is also described. No toxicity towards human erythrocytes was observed, proving their efficacy to be suitable for various biomedical applications.

Contents

Chapter 1: Introduction

Chapter 2: Covalent Coating on Textiles that can Switch from Bactericidal to Antifouling Properties

Chapter 3: Hydroxyapatite Loaded with Quaternary Chitosan-Silver Chloride Nanocomposites Selectively Kill Bacteria over Human Erythrocytes

Chapter 1

Introduction

1.1 Microbial Infection and Surfaces: A Potential Killer

Historically, infectious diseases have been the most important contributor to human morbidity and mortality. Rapid emergence of antimicrobial resistance to conventional antibiotics has become one of the biggest clinical threats.[1, 2] Formation of biofilm has further complicated the situation as antibiotics cannot penetrate them making them almost impossible to cure.[3-6]

Among the many ways by which infectious diseases spread, the contaminated surfaces are responsible for more than 50% of all microbial infections.[7] Contaminated surfaces can act as reservoirs of microbes which can lead to biofilm-associated infections of medical devices and implants.[8,9] Biofilms can be formed on abiotic surfaces (hospital walls, medical devices, implants etc.) as well as biotic surfaces (surgical sites, wounds, lungs, urinary tract, cardiac tissues, bones etc.).[10-13] Infections resulting from contaminated surfaces not only increase the patient's sufferings and healthcare costs but can also turn out to be fatal resulting in death of the patients.

1.2 Spreading of Infections by Surfaces

Upon being touched by a healthy individual, contaminated surfaces can spread infections. Various common community objects such as door knobs, linen, public telephones, children toys etc. when touched by infected people, pathogenic microorganism deposit onto surfaces. Coughing, sneezing, breathing or even talking spread out aerosolized moisture containing bacteria which deposit onto objects leading to surface contamination. When these contaminated surfaces are touched by healthy individuals, microbial infections are transmitted. [14-17] Infections caused by contaminated daily community objects from community are called as community acquired infections (CAIs).

Infectious microbes (e.g. bacteria, fungi, etc. are also prevalent in hospital atmosphere such as in the operating room, on surgical equipments, clothing worn by medical professionals, bacteria residing on the patient's skin, and bacteria already in the body.[18-20] In addition, increase in the usage of biomaterials and medical devices (such as catheters, cardiac pacemakers, hip implants, and contact lenses, etc.) conjugated with the contaminated surfaces can cause serious implant-associated infections.[21] Even though various aseptic techniques and sterilization procedures exist, pathogenic microorganisms are still found at the site of approximately 90% of all implants.

Infections caused by objects from hospital/healthcare settings are known as hospital-acquired infections (HAIs) or nosocomial infections. Almost 60% of all nosocomial infections are related to medical device and implants.[22] Device-related infection may result in substantial clinical complications, including death, as well as economic consequences such as increased healthcare costs generated by prolonged hospital stays or revision surgery. Many different sources contribute to the HAIs starting from surgical site infections (SSIs), urinary tract infections (UTIs), blood stream infections, pneumoniae, etc. and cost a heavy financial burden in addition to patient's sufferings. In the United States alone, recent estimates of direct costs for healthcare-associated infections were estimated to range from US$28 billion to $45 billion in 1 year.[23]

1.3 Pathogenesis of Device-Related Infection

Device-related infections result from the multifaceted interaction of bacterial, device, and host factors where the bacterial factors are probably the most important in the pathogenesis of device-associated infections. Different bacteria use different adhesins to colonize medical devices. The adherence of common Gram positive and Gram negative pathogens are discussed below.

***S. epidermidis*:** Adherence of this bacterium to the surface of the device is not a one-time phenomenon but ratheris an evolving process which initiates with a rapid attachment of bacterial cells to the surface of the device. This attachment to the surface is mediated either by nonspecific factors (such as surface tension, hydrophobicity, and electrostatic forces) or by specific adhesins (including the proteinaceous autolysin encoded by the atlE gene and the capsular polysaccharide intercellular adhesin [PSA] probably encoded by the ica operon).[24] This initial phase of *S. epidermidis* adherence is followed by an accumulative phase. During this phase bacteria form biofilm.[25]

S. aureus: Unlike *S. epidermidis*, well-defined adhesins are employed to adhere to one another and to the devices. Adherence of *S. aureus* appears to be more dependent on the presence of host-tissue ligands, including fibronectin, fibrinogen, and collagen. *S. aureus* adheres to such host-tissue ligands via genetically defined microbial surface proteins, which are commonly referred to as "microbial surface components recognizing adhesive matrix molecules" (MSCRAMM). The most

important MSCRAMMs include FnbpA and FnbpB, which bind to fibronectin. The role of MSCRAMM in the pathogenesis of device associated infections, however, is not clear and, at least in the case of orthopaedic device infection, has been a bit controversial.

***E.coli*:** *E. coli* is known to adhere to urological devices and cause infections. Adherence of *E. coli* to devices may be dependent on the location of the device and local predominance of certain bacterial strains, given that *E. coli* strains that express type 1 fimbriae prevail in the bladder, whereas *E. coli* strains that express P fimbriae usually infect the kidneys.

1.4 Different Strategies to tackle surface related infections

Antibacterial surfaces have emerged as a primary component of the global strategy to eliminate bacterial pathogens. Thanks to materials science and biotechnological advances, an extensive variety of options are now available to design surfaces with antibacterial properties. However, progress towards a more widespread use in clinical settings crucially depends on addressing the key issues. Various researchers have focused their research in developing antimicrobial surfaces that can prevent infections.[26,27] In this direction, three general strategies have been adopted; i) adhesion resistance (non-fouling strategy), ii) biocide releasing (release-based strategy) and iii) contact killing (contact-based strategy).[28]

In adhesion resistant approach, surfaces owing to its cell-repellent nature, hinder the adherence of microbial cells. Anti-adhesion surfaces thus prevent the earliest step of biofilm formation. Bacterial adhesion at biomaterial surfaces occurs in a two-stage model: an initial, rapid and reversible stage, mediated by non-specific physicochemical interactions. This stage is followed by a secondary ‘locking’ stage. Surface immobilization of molecules that can resist protein adsorption, such as PEG and zwitterionic compounds, have shown tremendous anti-adhesion properties *in-vitro*.

Release-based coatings function by leaching the loaded antimicrobials, killing both adhered as well as adjacent microbes. Such coatings exert their antibacterial activity by leaching loaded antibacterial compounds over time, which allows killing of both adhered and adjacent planktonic bacteria. The release of incorporated antibacterial agents is achieved by diffusion into the aqueous medium, erosion/degradation, or hydrolysis of covalent bonds.[28] Compared with

traditional antibiotic delivery methods, direct elution from the material surface can effectively deliver a antibacterial agent concentration locally, without exceeding systemic toxicity or ecotoxicity limits. It provides a controlled antibacterial activity only at the site of infection minimizing the development of resistance and avoiding potentially harmful systemic repercussions. However, because release-based surfaces have inherently limited reservoirs of antibacterial agents, their action is ultimately only temporary.

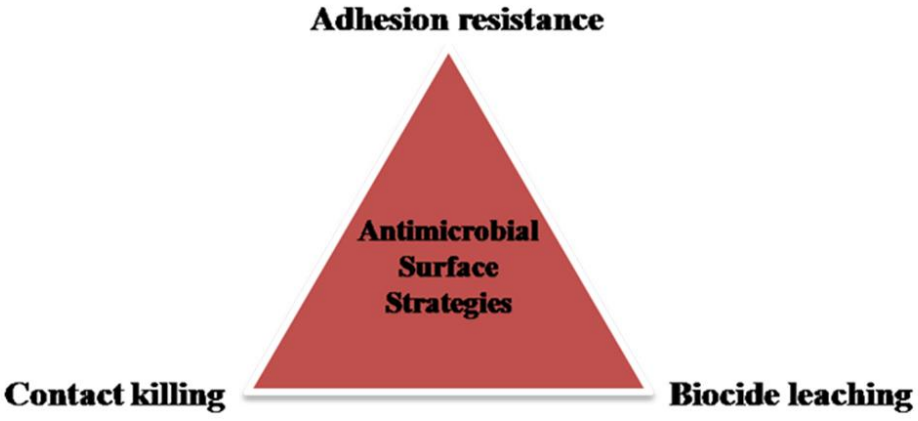

Figure 1.1: Three chief strategies for designing antibacterial surfaces (Figure was adapted from reference 17).

In contact killing strategy, microbes are killed upon contact with the coated surfaces. Contact-killing surfaces have been developed to circumvent the reservoir exhaustion issue of release-based materials.[29] In this approach, antimicrobial compounds are anchored to the material surface. To anchor antimicrobials to surfaces, both covalent and non-covalent surface-modifications have been adopted. Adhered bacteria are believed to be killed due to disruption of their cell membrane by the attached compounds, reaching across the microbial envelope, owing to the long tethering hydrophobic chains.[26] Because the main mechanisms of action are based on membrane interactions, such as physical lysing or charge disruption, the most effective compounds for contact-killing coatings have been either cationic compounds (QACs, chitosan, AMPs, etc.) or enzymes.[31]

1.4.1 Adhesion Resistant and Antifouling Surfaces

Antifouling surface focuses on inhibiting microbial adhesion or reducing the capacity of microbes to adhere on the surface. Different materials are employed as antifouling coatings. One well established method for preventing microbial adhesion to surfaces is to covalently attached them with a layer of poly (ethylene glycol), PEG.[32] Recently, polymers with zwitterionic head groups such as poly(phosphorylcholine), poly (sulfobetaine) and poly(carboxybetaine) have been shown to inhibit bacterial adhesion and biofilm formation on surfaces. [33,34] It is postulated that the zwitterionic head can associate a large amount of water, making the material heavily hydrophilic leading to reversible interactions between the incident microbes and the surface-discouraging their adhesion.

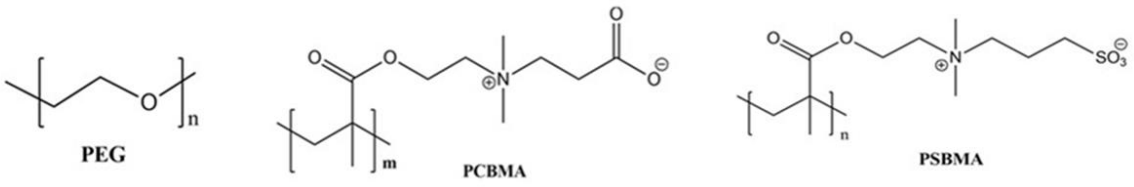

Figure 1.2: Various anti-adhesion polymers used in developing nonfouling surface. PEG: poly (ethylene glycol); PCBMA: poly(carboxybetaine methacrylate); PSBMA: poly(sulfobetaine-methacrylate)

These zwitterionic surfaces was shown to be promising for coating medical devices, because of their biomimetic nature which firstly provides biocompatibility by reducing attachment of human cells to the device and secondly offers protection against bacterial biofilm formation. However, these types of surfaces, do not fully address the problem of microbial contamination as they have no antimicrobial functionality and hence are intrinsically inactive against pathogens. Though they can resist their adherence, once infected, they cannot kill the microbes.

1.4.2 Biocide Releasing Surfaces

The release-based approach is focused on biocide leaching, in which antimicrobial compounds are released and diffused over time from a material surface, inducing death either of nearby (but non-adhered) bacteria or of adhered bacteria.[22] A variety of active antimicrobials such as antibiotics,

metal salts or nanoparticle, bioactive species (e.g., phage virus), etc. has been impregnated onto surfaces to develop biocide-releasing antimicrobial surfaces.[7] One of the most heavily marketed and most widespread products for suppressing microbial growth is Microban incorporating Triclosan (5-chloro-2-(2,4-dichlorophenoxy)-phenol) into a surface. Silver has long been known to be an antimicrobial and the metal ions (Ag^+) have a significant antimicrobial activity finding its use in various commercial aspects. AgION Technology's AgION™ and AcryMed's SilvaGard™ are two of the most well-known commercial coating products which rely on the diffusion of Ag^+ ions from the substrate material and inactivate the microorganisms. But a possible drawback of silver-based antimicrobials is the cytotoxicity of Ag^+ ions towards mammalian cells. Like silver, copper has long been considered to be a hygienic material.[35] Another important way of developing release-active surfaces is by immobilizing bacteriophage viruses that infect prokaryotic cells. Developments of a phage containing wound dressing, hydrogel-coated silicone catheter, etc. with lytic bacteriophages have been well documented.[36]

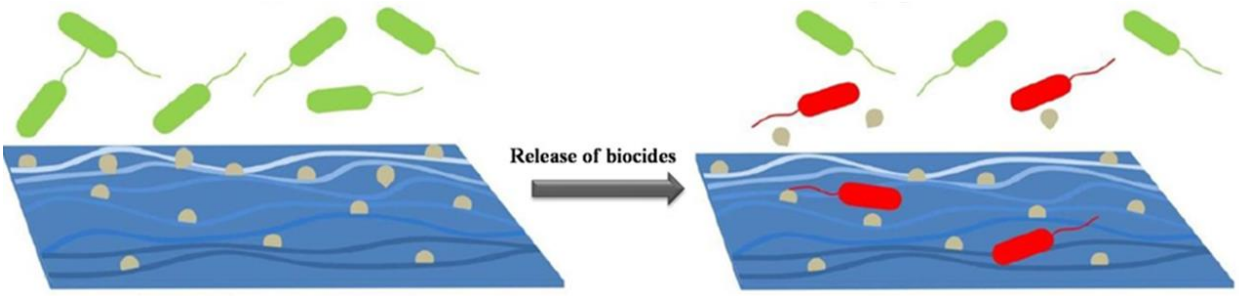

Figure 1.3: Schematic representation of a release-based antimicrobial surface.

The overall timeframe and kinetics of antibacterial delivery are highly application-dependent. It provides antibacterial protection during the early post-operation period, which is considered the most critical stage for infection risk, and limits the development of bacterial resistance.

However, for implanted devices, surfaces should maintain their antibacterial properties until integration with the surrounding tissues, which can take up to several months, to prevent bacterial colonization from the hematogenous route.[37] Long-term release is also needed for revision surgeries, where implants are already in a contaminated tissue region[22] To date, designing coatings that maintain released antibacterial compounds levels within the therapeutic window,

sufficient to kill bacteria but low enough to limit cytotoxicity toward eukaryotes, remains a significant challenge. Innovative approaches to control and extend release kinetics are therefore necessary to generate new solutions and products.

1.4.3 Contact Killing

1.4.3.1 Non-covalent Coating

Quaternized polymers are widely used which were organo-soluble and water-insoluble to paint surfaces rendering them antimicrobial. A quaternized polyethyleneimine (PEI) derivative *N*-hexyl, *N*-methyl-PEI –based coating was developed on various surfaces such glass or polyethylene surfaces were capable to kill airborne *S. aureus*. However, this antimicrobial surface developed using this shorter alkyl chain bearing PEI derivative was not permanent. The deposited antibacterial polymer was found to leach out from the.[38] A new antimicrobial surfaces with higher hydrophobicity bearing polymer was hypothesised to strengthen the intermolecular attractions and thus lesser tendency to leach out from the surface. Later on, PEI derivatives bearing higher hydrophobic moieties were synthesized to tackle this issue.[39-41]

Layer by layer (LbL) assembly is also employed to coat surfaces with solutions of two differently charged compounds in an alternative manner. An LbL assembly made up from bactericidal and virucidal cationic PEI derivative by using the anionic poly (acrylic acid) was reported.[42,43] The surface showed potent efficacy against both airborne and waterborne *E. coli* and *S. aureus* including virucidal activity against influenza virus with no cytotoxicity towards mammalian cells.[44]

Our group has further investigated a detailed structure-activity relationship of a series of polyethylenimine based quaternized polymer-coated surfaces. A series of quaternized polyethylenimine were prepared by using the precursor polymers of various molecular weights. PEI derivatives with varied degree of quaternization were prepared using different long chain alkyl bromides.[45] The resulting polymers were water insoluble and organo-soluble. Various surfaces were coated by easily dissolving the compound in various organic solvent. The surface coated with these polymers displayed activity against various pathogenic bacteria including drug-resistant

superbugs MRSA and VRE and against pathogenic fungi such as *Candida spp.* and *Cryptococcus spp*.[45]

Recently, our group has reported another class of antimicrobial surfaces, where quaternized chitin derivatives were used. [46] The water-insoluble and organo-soluble antibacterial chitin derivatives were prepared by selective quaternization at C-6 position of the sugar unit by using various *N*,*N*-dimethylalkylamines (such as *N*,*N*-dimethyltetradecylamine, *N*,*N*-dimethylhexadecylamine). By dissolving the polymers in methanol, it was coated on various surfaces such as polystyrene plates, glass slides or cover glasses by employing brush, dip or spin-coating or drop casting. Polystyrene plates coated with these polymers showed potent activity against both drug-sensitive and drug-resistant bacteria (MRSA and VRE) with minimal toxicity against mammalian cells (RBCs and embryo kidney cells).[46]

1.4.3.2 Covalent Coating

Klibanov and co-workers developed a covalent coating of by immobilizing poly- (4-vinyl-*N*-alkylpyridinium bromide) on glass.[29] Russel and co-workers developed an antimicrobial polymer directly on the surface by employing atom transfer radical polymerization (ATRP).[47] These reports involve complicated and sophisticated reactions on the surfaces. To this aim, researchers are immensely focusing on the development of coating procedure avoiding complicated techniques. Recent research has resulted in the development of polymers functionalized with active linkers which can bind the polymeric structure to various surfaces. Incorporation of such linkers in the polymeric architecture paves an easier way to coat the polymers on the surfaces which requires only one-step fabrication. Locklin and co-workers have developed coating involving benzophenone moieties which render UV curable property to the coating material.[48-50] Klibanov and co-workers have also reported a covalent coating incorporating a photoactive linker 6-(4′-azido-2-nitrophenylamino) hexanoyl into branched polyethyleneimine.[51] Upon incubation of water borne pathogens *E. coli and S. aureus* with the photo-coated cotton, no viable bacteria were detected. Dopamine has also been utilized as an anchoring agent.[52-56] Various dopamine-incorporated antimicrobial polymeric coatings are reported in the recent past. Yang and co-workers

have developed a one-step polycarbonate-based coating which employs dopamine as a linker.[52] The brush-like polycarbonates when coated on surface, was active against *S. aureus* and *E. coli*.

1.5 Scope of the Thesis

Because of the ever-growing demand for healthy living, there is a keen interest in materials capable of killing harmful microorganisms. Increased usage of of healthcare materials conjugated with the emergence and spread of resistant microbes has resulted in higher risk of surface associated infections. To tackle such infections, various modified antimicrobial surfaces are designed and are used. Surface treatment can be done in different modification principles. Cationic surfaces can inactive microbes on contact. Polyethylene glycol-based various anti-adherent surfaces are also developed to resist the attachment of bacteria to surfaces. Several surfaces are developed which kills bacteria by releasing antimicrobials from the surface. But several limitations are there to these methods. Anti-adhesive surfaces are mostly intrinsically inactive. Also, polymer matrices used as reservoirs for releasing antimicrobials are not active against pathogens. Contact active surfaces suffer from fouling, deposition of dead bacterial cells, proteins on the surfaces which spoil the surface making it ineffective with time.

The aim of this thesis is to develop antimicrobial materials to address the above mentioned limitations of currently existing strategies. In Chapter 2, a covalent coating on cotton textile is developed based on UV-active linker benzophenone. The one step simple fabrication of antimicrobial textile is discussed with its detailed antimicrobial efficacy. The coating on the textile upon degradation transforms into zwitterionic form, imparting antifouling property to the surface. The coating was seen to adhere lower number of bacteria upon degradation making the textile coating switch from bactericidal to antifouling one.

Chapter 3 reports the simple *in-situ* synthesis of dual-action polymer-silver chloride nanocomposites from an aqueous solution of a quaternary chitosan derivative and a silver salt. Both the polymer and the nanoparticles are active against pathogens. The efficacies of the nanocomposites against both Gram-positive and Gram-negative bacteria including the drug-resistant pathogens are discussed. The nanocomposites were found to be highly active against Gram-negative pathogens, owing to the presence of silver chloride nanoparticles. Hydroxyapatite, a well known material for orthopaedic applications, was loaded with the most active nanocomposite **QAm_1-Ag_1.** The loaded material was active against Gram-positive and Gram-

negative pathogens with negligible *in-vitro* toxicity towards human erythrocytes. The materials are efficacious for different biomedical applications.

References

(1) Willyard, C. *Nature* **2017**, *28*, 543.

(2) Brown, E. D.; Wright, G. D. *Nature* **2016**, *529*, 336.

(3) Stewart, P. S.; Costerton, J. W. *Lancet* **2001**, *358*, 135.

(4) Parsek, M. R.; Singh, P. K. *Annu. Rev. Microbiol*. **2003**, *57*, 677.

(5) Hall-Stoodley, L.; Costerton, J. W.; Stoodley, P. *Nat. Rev. Microbiol.* **2004**, *2*, 95.

(6) McDougald, D.; Rice, S. A.; Barraud, N.; Steinberg, P. D.; Kjelleberg, S. *Nat. Rev. Microbiol.* **2012**, *10*, 39.

(7) Page, K.; Wilson, M.; Parkin, I. P. *J. Mater. Chem.* **2009,** *19*, 3819.

(8) Darouiche, R. O. *N. Engl. J. Med.* **2004,** *350*, 1422.

(9) Bjarnsholt, T.; Ciofu, O.; Molin, S.; Givskov, M.; Hoiby, N. *Nat. Rev. Drug. Discov.* **2013,** *12*, 791.

(10) Trampuz, A.; Piper, K. E.; Jacobson, M. J.; Hanssen, A. D.; Unni, K. K.; Osmon, D. R.; Mandrekar, J. N.; Cockerill, F. R.; Steckelberg, J. M.; Greenleaf, J. F.; Patel. R. *N. Engl. J. Med.* **2007**, *357*, 654.

(11) Imamura, Y.; Chandra, J.; Mukherjee, P. K.; Lattif, A. A.; Szczotka-Flynn, L. B.; Pearlman, E.; Lass, J. H.; O'Donnell, K.; Ghannoum, M. A. *Antimicrob. Agents Chemother.* **2008**, *52*, 171.

(12) Costerton, J. W.; Stewart, P. S.; Greenberg, E. P. *Science* **1999**, *284*, 1318.

(13) Koo, H.; Allan, R. N.; Howlin, R. P.; Stoodley, P.; Hall-Stoodley, L. *Nat. Rev. Microbiol.* **2017**, *15*, 740.

(14) Oie, S.; Hosokawa, I.; Kamiya, A. *J. Hosp. Infect.* **2002**, *51*, 140.

(15) Dietze, B.; Rath, A.; Wendt, C.; Martiny, H. *J. Hosp. Infect.* **2001**, *49*, 255.

(16) Banerjee, D.; Fraise, A.; Chana, K. *J. Hosp. Infect.* **1999**, *43*, 73.

(17) Bures, S.; Fishbain, J. T.; Uyehara, C. F. T.; Parker, J. M.; Berg, B. W. *Am. J. Infect. Control* **2000**, *28*, 465.

(18) Talon, D. *J. Hosp. Infect.* **1999,** *43*, 13.

(19) Hota, B. *Clin. Infect. Dis.* **2004,** *39*, 1182.

(20) Neely, A. N.; Maley, M. P. *J. Clin. Microbiol.* **2000,** *38*, 724.

(21) Darouiche, R. O. *N. Engl. J. Med.* **2004,** *350*, 1422.

(22) Hetrick, E. M.; Schoenfisch, M. H. *Chem. Soc. Rev.* **2006,** *35*, 780.

(23) Salwiczek, M.; Qu, Y.; Gardiner, J.; Strugnell, R. A.; Lithgow, T.; McLean, K. M.; Thissen, H. *Trends Biotechnol.* **2014,** *32*, 82.

(24) Rupp ME, Ulphani JS, Fey PD, Bartscht K, Mack D. *Infect. Immun.* **1999**, *67*, 2627.

(25) Greene C, McDevitt D, Francois P, Vaudaux PE, Lew DP, Foster TJ. *Mol. Microbiol*. **1995**, *17*, 1143.

(26) Lewis, K.; Klibanov, A. M. *Trends in Biotechnology* **2005,** *23*, 343.

(27) Campoccia, D.; Montanaro, L.; Arciola, C. R. *Biomaterials* **2013,** *34*, 8533.

(28) Lichter, J. A.; Van Vliet, K. J.; Rubner, M. F. *Macromolecules* **2009,** *42*, 8573.

(29) Tiller, J.C.; Klibanov, A. M. *Proc. Natl. Acad. Sci. U.S.A.* **2001,** *98*, 5981.

(30) Green, J-B.D. *Biointerphases* **2011**, *6*, MR13.

(31) Ostuni, E.; Chapman, R. G.; Liang, M. N.; Meluleni, G.; Pier, G.; Ingber, D. E.; Whitesides, G. M. *Langmuir* **2001**, *17*, 6336.

(32) Cheng, G.; Zhang, Z.; Chen, S.; Bryers, J. D.; Jiang, S. *Biomaterials* **2007**, *28*, 4192.

(33) Hirota, K.; Murakami, K.; Nemoto, K.; Miyake, Y. *Fems Microbiology Letters* **2005**, *248*, 37-45.

(34) Weaver, L.; Michels, H. T.; Keevil, C. W. *J.Hosp. Infect.* **2008**, *68*, 145.

(35) Markoishvili, K.; Tsitlanadze, G.; Katsarava, R.; Morris, J. G.; Sulakvelidze, A. *Int. J. Dermatol.* **2002**, *41*, 453.

(36) Curtin, J. J.; Donlan, R. M. *Antimicrob. Agents Chemother.* **2006**, *50*, 1268.

(37) Busscher, H.J. et al. *Sci. Transl. Med.* **2012**,*4*, 153rv110.

(38) Park, D.; Wang, J.; Klibanov, A. M. *Biotechnol. Prog.* **2006,** *22*, 584.

(39) Haldar, J.; An, D.; Alvarez de Cienfuegos, L.; Chen, J.; Klibanov, A. M. *Proc. Natl. Acad. Sci. U. S. A.* **2006**, *103*, 17667.

(40) Haldar, J.; Chen, J.; Tumpey, T. M.; Gubareva, L. V.; Klibanov, A. M. *Biotechnol. Lett.* **2008**, *30*, 475.

(41) Haldar, J.; Weight, A. K.; Klibanov, A. M. *Nat. Protoc.* **2007**, *2*, 2412.

(42) Wong, S. Y.; Li, Q.; Veselinovic, J.; Kim, B. S.; Klibanov, A. M.; Hammond, P. T. *Biomaterials.* **2010**, *31*, 4079.

(43) Wong, S. Y.; Han, L.; Timachova, K.; Veselinovic, J.; Hyder, M. N.; Ortiz, C.; Klibanov, A. M.; Hammond, P. T. *Biomacromolecules* **2012,** *13*,719.

(44) Schaer, T. P.; Stewart, S.; Hsu, B. B.; Klibanov, A. M. *Biomaterials* **2012,** *33*, 1245.

(45) Hoque, J.; Akkapeddi, P.; Yadav, V.; Manjunath, G. B.; Uppu, D. S.; Konai, M. M.; Yarlagadda, V.; Sanyal, K.; Haldar, J. *ACS Appl. Mater. Interfaces.* **2015**, *7*, 1804.

(46) Hoque, J.; Akkapeddi, P.; Ghosh, C.; Uppu, D. S.; Haldar, J. *ACS Appl. Mater. Interfaces.* **2016**, *8*, 29298.

(47) Lee, S. B.; Koepsel, R. R.; Morley, S. W.; Matyjaszewski, K.; Sun, Y.; Russell, A. J. *Biomacromolecules* **2004**, *5*, 877.

(48) Dhende, V. P.; Samanta, S.; Jones, D. M.; Hardin, I. R.; Locklin, J. *ACS Appl. Mater. Interfaces* **2011**, *3*, 2830.

(49) Liu, Q.; Singha, P.; Handa, H.; Locklin, J. *Langmuir* **2017**, *33*, 13105.

(50) Gao, J.; White, E. M.; Liu, Q.; Locklin, J. *ACS Appl. Mater. Interfaces*. **2017**, **9**, 7745.

(51) Hsu, B. B.; Klibanov, A. M. *Biomacromolecules* **2011**, *12*, 6.

(52) Chuan Yang, C.; Ding, X.; Ono, R. J.; Lee, H.; Hsu, L. Y.; Tong, Y. W.; Hedrick, J.; Yang, Y. Y *Adv. Mater.* **2014**, *26*, 7346.

(53) Lee, B. P.; Messersmith, P. B.; Israelachvili, J. N.; Waite, J. H. *Annu. Rev. Mater. Res.* **2011**, *41*, 99.

(54) Lee, H.; Dellatore, S. M.; Miller, W. M.; Messersmith, P. B. *Science* **2007**, *318*, 426.

(55) Sileika, T. S.; Kim, H. D.; Maniak, P.; Messersmith, P. B. *ACS Appl. Mater. Interfaces* **2011**, *3*, 4602-4610.

(56) Han, H.; Wu, J.; Avery, C. W.; Mizutani, M.; Jiang, X. Kamigaito, M.; Chen, Z.; Xi, C.; Kuroda, K. *Langmuir* **2011**, *27*, 4010-4019.

Chapter 2

Covalent Coating on Textiles that can Switch from Bactericidal to Antifouling Properties

Abstract

This chapter describes the synthesis and characterization of cationic benzophenone derivatives with non-degradable aliphatic chains and degradable chains bearing ester and amide moieties. It also reports the development of a zwitterionic analogue. Antibacterial efficacy of these compounds has been investigated in solution phase against various Gram-positive and Gram-negative bacteria including drug-resistant bacteria methicillin-resistant *Staphylococcus aureus* (MRSA), vancomycin-resistant *Enterococcus faecium* (VRE). They were also showed to have potent activity against various clinically isolated strains. Compounds **6** (ester derivative) and **7** (amide derivative) were covalently coated onto cotton surfaces from their aqueous solutions by UV irradiation at ~ 365 nm. The coated cotton showed excellent activity against various Gram-positive pathogens. Cottons coated with compound **6** and **7** showed complete killing of MRSA in 1 h and 30 min respectively. Cottons coated with the zwitterionic compound **9** showed reduced adhesion of bacteria to the textile surfaces.

2.1 Introduction

Microbial infection poses serious threat to for commercial applications many materials such as textiles, food packaging and storage, shoe industry, medical devices, water purification, and dental surgery equipment.[1-4] Thus, development of a new methodology for surface immobilization of antimicrobial polymers with well-defined properties is necessary. This can be accomplished by anchoring various classes of antimicrobials (such as, antibiotics, antimicrobial peptide, quaternary ammonium compounds, etc.) to surfaces.[5-9] A surface can be modified either by covalently immobilizing an antimicrobial to it or physically adhering any bactericidal agent on its surface. Non-covalent approach is based on painting of water-insoluble and organo-soluble antimicrobial polymers on different surfaces. This principle makes the preparation of antimicrobial surfaces simpler, where coating procedure is as simple as painting. Klibanov and co-workers have played a pioneering role in this direction.[10-18] But leaching of antimicrobials from the modified surfaces can decrease their usability quotient which means that antimicrobial coatings need to be immobilized irreversibly or covalently to the surfaces for durable and long-lasting activity. Various groups have put the initial efforts to develop non-leaching permanent antimicrobial coatings on different surfaces. A covalent coating by immobilizing poly- (4-vinyl-N-alkyl pyridinium bromide) on glass.[19] Development of an antimicrobial polymer directly on the surface by employing atom transfer radical polymerization (ATRP) has also been reported.[20] Even though the antimicrobials are anchored covalently to the surfaces, these reports involve reactions on the surfaces which are complicated and require sophisticated techniques. To this aim, researchers are immensely focusing on the development of a coating procedure which does not employ reactions involving the surfaces thereby avoiding complicated techniques. Recent research has resulted in the development of polymers or small molecules functionalized with active linkers which can bind the molecule to various surfaces. Incorporation of such linkers paves an easier way to coat the surfaces by only one-step fabrication. Use of benzophenone (BP) as an anchoring agent is well known in literature.[21-23] The linking ability of BP is furnished by abstraction of a hydrogen from a suitable hydrogen donor which has been studied extensively and has been employed in different applications for many years.[24-30] BP serves as an ideal cross-linking agent because it can be activated using mild UV light (345-365 nm), which avoids the oxidative damage of the surface which could happen upon exposure to higher energy UV. BP

moiety is chemically more robust than other organic cross-linkers. It undergoes reaction preferentially with C-H bonds in different chemical environments. Upon exposure of UV-light, an n-π* transition takes place forming a bi-radical triplet excited state. This bi-radical triplet state can effect abstraction of a hydrogen atom from a neighboring aliphatic C-H group thereby forming a new C-C bond.[31]

Antimicrobial coatings developed by immobilizing antibacterial agents are generally non-degradable and toxic.[32,33] The long-term exposure of non-degradable coatings might result in unpredictable cytotoxicity hindering implant-tissue integration. Furthermore, cationic coatings suffer from accumulation of dead bacterial cells on them. This dead cell accumulation leads to fouling of surfaces. Microbes can then adhere to this fouled surface further colonizing and forming biofilms. Hence, to be suitable for biomedical applications, an antimicrobial coating should kill microbes and prevent their colonization on medical devices or implants for required period of time and, where applicable, then transformed into an inactive non-toxic zwitterionic structure which will exert antifouling property. This chapter deals with the design and development of a charge-switchable antimicrobial coating on cotton textile by UV irradiation based on water-soluble cationic benzophenone derivatives bearing hydrolysable amide or ester groups in the side alkyl chain, which upon hydrolysis in presence of acid or enzymes, transforms into non-toxic and antifouling zwitterionic moiety (Scheme 2.1). The cotton textiles coated with the cationic degradable derivatives are checked for their activity against various Gram-positive pathogens. Upon degradation, the nature of the coating changes from cationic to zwitterionic one, which is checked for its antifouling property (Scheme 2.2). Bactericidal killing kinetics, non-leaching activity is also described and discussed.

2.2 Experimental Section

2.2.1 Materials and Instrumentation

All the solvents were of reagent grade, which were distilled and dried before its uses. All the reagents were purchased from Sigma-Aldrich, S.D. Fine, and Spectrochem were used without further purification. Analytical thin layer chromatography (TLC) was performed on E. Merck TLC plates pre-coated with silica gel 60 F_{254} and visualization was carried out using UV light and Iodine. Column chromatography was performed on silica gel (60-120 mesh) using different

ratio of chloroform and methanol solvent system. Nuclear magnetic resonance spectra were recorded on Bruker (AV-400) 400 MHz spectrometer in deuterated solvents. Mass spectra were obtained using 6538-UHD Accurate mass Q-TOF LC-MS instrument. For optical density measurement Tecan InfinitePro series M200 Microplate Reader was used. Bacterial strains, *S. aureus* (MTCC 737), *P. aureginosa* (MTCC 424)*E. coli* (MTCC 443) were purchased from MTCC (Chandigarh, India). Methicillin-resistant *S. aureus* (ATCC 33591), *Enterococcus faecium* (ATCC 19634), vancomycin-resistant *Enterococcus faecium* (ATCC 51559), and *Klebsiella pneumoniae* (ATCC 700603) were obtained from ATCC (Rockville, MD, USA). Unbleached cotton was bought from local market in Bengaluru.

2.2.2 Synthesis and Characterization

2.2.2.1 Reaction Scheme

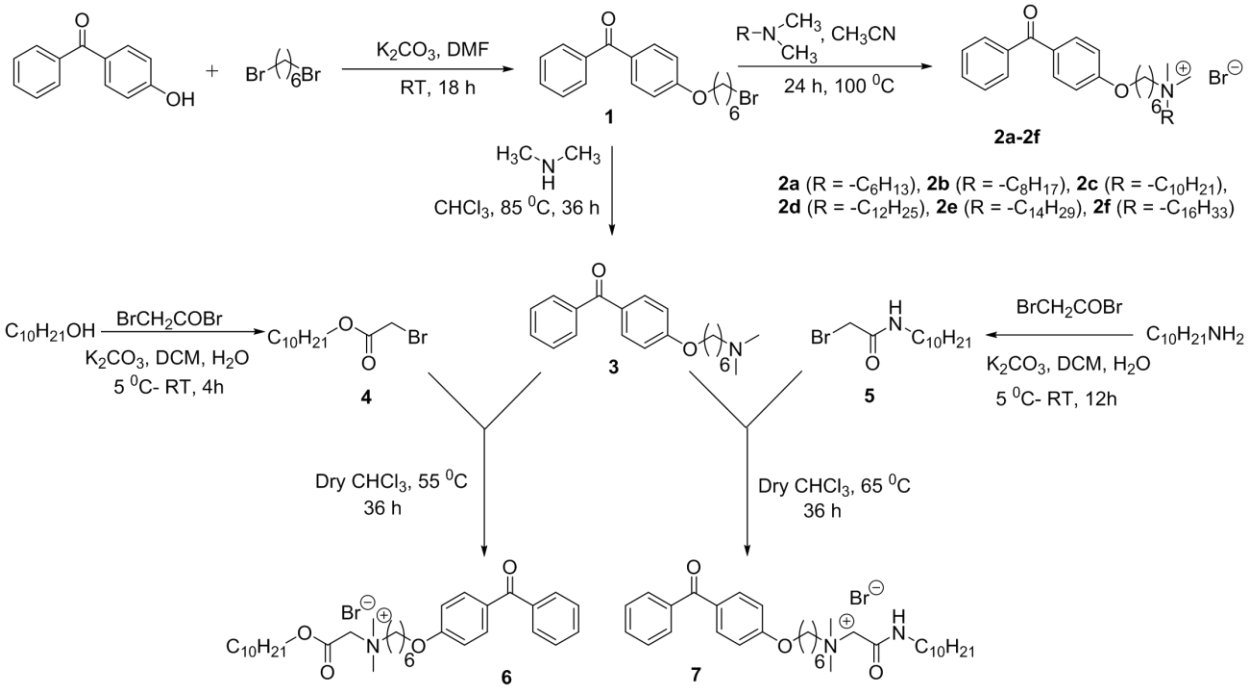

Scheme 2.1: Synthesis of cationic benzophenone derivatives.

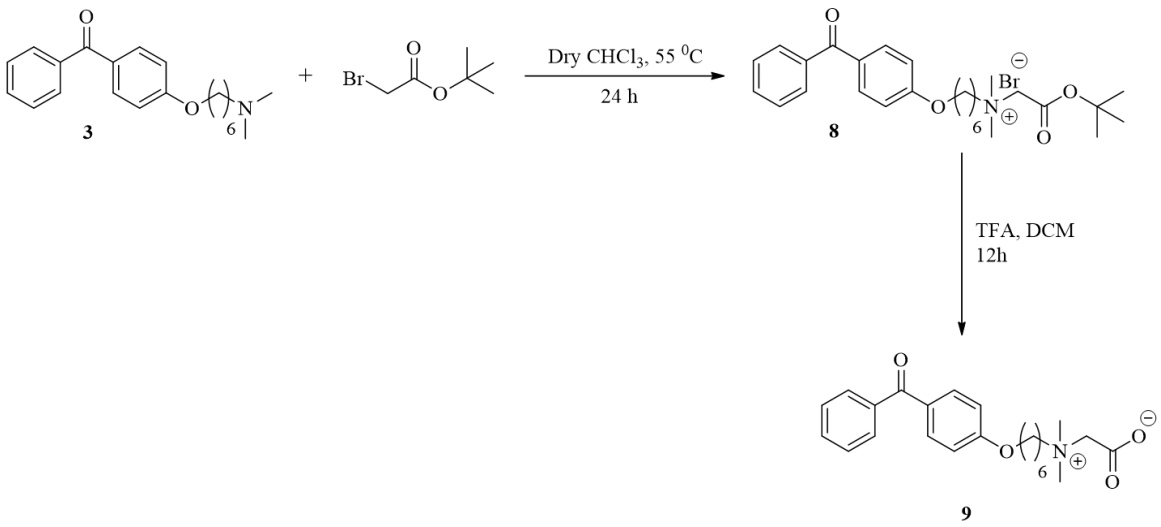

Scheme 2.2: Synthesis of zwitterionic benzophenone derivative.

2.2.2.2 Synthetic Protocols and Characterization

Procedure for synthesizing (4-((6-bromohexyl)oxy)phenyl)(phenyl)methanone (1): 4-Hydroxy benzophenone (1 equiv), 1,6 dibromohexane (1.5 equiv), potassium carbonate (1.5 equiv) and dry DMF were stirred at room temperature for 18 h under argon atmosphere.The reaction mixture was poured into ice-water mixture (300 mL) and extracted with $CHCl_3$. The organic layer was collected and the solvent was removed under reduced pressure. The crude product was purified on a silica gel column by using 50:1 hexane: ethyl acetate mixture. (74 % yield) ^{1}H-NMR ($CDCl_3$, 400 MHz) δ/ppm: 7.820-7.798 (d, Ar-H), 7.758-7.775(d, Ar-H), 7.738,7.735(d, Ar-H); 7.584-7.577(t, Ar-H), 6.965-6.931(d, Ar-H), 4.066-4.035(t, O-C*H*$_2$).

General procedure for synthesizing 2a-2f: Compound **1** was taken (1 equiv) and the *N*,*N* dimethyl alkyl amine (2 eqv, R= -C_6H_{13}, -C_8H_{17}, -$C_{10}H_{21}$, -$C_{12}H_{25}$, -$C_{14}H_{29}$, -$C_{16}H_{33}$) in dry CH_3CN and stirred for 24h in a screw top sealed pressure tube at 100^0 C. Precipitation was done with diethyl ether.

(*N*-(6-(4-benzoylphenoxy)hexyl)-*N*,*N*-dimethylhexan-1-aminium bromide), (2a): (85% yield) ^{1}H-NMR ($CDCl_3$, 400MHz) δ/ppm: 7.820-7.798 (d, Ar-H), 7.758-7.775(d, Ar-H), 7.738,7.735(d, Ar-H); 7.584-7.577(t, Ar-H), 6.965-6.931(d, Ar-H), 4.066-4.035(t, O-C*H*$_2$), 3.641-3.619(m, N-C*H*$_2$-CH_2-), 3.598-3.497(m, N-*CH*$_2$-CH_2-), 3.396(s, N-(*CH*$_3$)$_2$), 1.859-1.502(m), 0.956-0.889 (t, -*CH*$_3$); HRMS (m/z):calculated : 410.3054; observed : 410.30175.

(*N*-(6-(4-benzoylphenoxy) hexyl)-*N,N*-dimethyloctan-1-aminium bromide), (2b): (77% yield) ^{1}H-NMR ($CDCl_3$, 400 MHz) δ/ppm: 7.820-7.798(d, Ar-H), 7.758-7.775(d, Ar-H), 7.738-7.735(d, Ar-H), 7.584-7.577(t, Ar-H), 6.965-6.931(d, Ar-H), 4.066-4.035 (t, O-C*H*$_2$), 3.641-3.619(m, N-C*H*$_2$-CH_2-), 3.598-3.497(m, N-*CH*$_2$-CH_2-), 3.389 (s, N-(*CH*$_3$)$_2$), 1.859-1.502(m), 0.889 (t, -C*H*$_3$); HRMS (m/z):calculated: 438.3667; observed : 438.32262.

(*N*-(6-(4-benzoylphenoxy) hexyl)-*N,N*-dimethyldecan-1-aminium bromide), (2c): (90% yield) ^{1}H-NMR ($CDCl_3$, 400 MHz) δ/ppm: 7.820-7.798(d, Ar-H), 7.758-7.775(d, Ar-H), 7.738-7.735 (d, Ar-H), 7.584-7.577(t, Ar-H), 6.965-6.931(d, Ar-H), 4.066-4.035(t, O-*CH*$_2$), 3.641-3.619(m, N-*CH*$_2$-CH_2-), 3.598-3.497 (m, N-*CH*$_2$-CH_2-), 3.386(s, N-(*CH*$_3$)$_2$), 1.859-1.502(m, 24H), 0.889-0.872(t, -C*H*$_3$)**;** HRMS (m/z): calculated: 466.3680; observed: 466.35401.

(*N*-(6-(4-benzoylphenoxy) hexyl)-*N,N*-dimethyldodecan-1-aminium bromide), (2d): (92% yield) ^{1}H-NMR ($CDCl_3$, 400M Hz) δ/ppm: 7.820-7.798(d, Ar-H), 7.758-7.775(d, Ar-H), 7.738-7.735(d, Ar-H), 7.584-7.577(t, Ar-H), 6.965-6.931 (d, Ar-H), 4.066-4.035(t, O-C*H*$_2$), 3.641-3.619(m, N-C*H*$_2$-CH_2), 3.598-3.497(m, N-C*H*$_2$-CH_2-), 3.389(s, N-(C*H*$_3$)$_2$), 1.859-1.502(m), 0.893-0.837 (t, -C*H*$_3$)**;** HRMS (m/z):calculated: 494.3993; observed: 494.38407.

(*N*-(6-(4-benzoylphenoxy) hexyl)-*N,N*-dimethyltetradecan-1-aminium bromide), (2e): (88% yield) ^{1}H- NMR ($CDCl_3$, 400 MHz) δ/ppm: 7.820-7.798 (d, Ar-H), 7.758-7.775 (d, Ar-H), 7.738-7.735 (d, Ar-H), 7.584-7.577(t, Ar-H), 6.965-6.931(d, Ar-H), 4.066-4.035(t, O-C*H*$_2$), 3.641-3.619 (m, N-C*H*$_2$-CH_2-), 3.598-3.497(m, N-C*H*$_2$-CH_2-), 3.389(s, N-(C*H*$_3$)$_2$), 1.859-1.502(m), 0.889 (t, -C*H*$_3$)**;** HRMS (m/z):calculated: 522.4306; observed: 522.43276.

(*N*-(6-(4-benzoylphenoxy) hexyl)-*N,N*-dimethylhexadecan-1-aminium bromide), (2f): (70% yield) ^{1}H-NMR ($CDCl_3$, 400 MHz) δ/ppm: 7.820-7.798 (d, Ar-H), 7.758-7.775 (d, Ar-H), 7.738-7.735 (d, Ar-H), 7.584-7.577(t, Ar-H), 6.965-6.931(d, Ar-H), 4.066-4.035 (t, O-C*H*$_2$), 3.641-3.619 (m, N-C*H*$_2$-CH_2-), 3.598-3.497 (d, N-C*H*$_2$-CH_2), 3.369(s, N-(C*H*$_3$)$_2$), 1.859-1.502(m), 0.889(t, -C*H*$_3$)**;** HRMS(m/z): calculated: 550.4619; observed: 550.70390.

Procedure for synthesizing (4-((6-(dimethylamino)hexyl)oxy)phenyl)(phenyl)methanone, (3): Compound **1** was dissolved in dry chloroform (40 mL) in a screw-top pressure tube. Dry $NHMe_2$ gas was collected to the solution at 0 °C until the volume of the resulting solution was roughly doubled (80 mL). Then the reaction mixture was stirred for 24 h at 80 °C overnight.

After the reaction, the pressure tube was cooled and the reaction mixture was transferred to a round bottom flask and the final volume of the reaction mixture was made to 150 mL by adding chloroform. The unreacted gas was removed carefully by heating slowly until wet litmus paper no longer turns blue on exposure to the emerging vapors. The solution was 100 mL) in order to deprotonate the products. Finally,×washed with 2 M KOH solution (3 the organic layer was passed through anhydrous Na_2SO_4 and was dried to give brownish-yellow coloured liquid. (85% yield) ^{1}H-NMR ($CDCl_3$, 400 MHz) δ/ppm: 7.82-6.93(Ar-H), 4.04(Ph-O-C*H*$_2$-), 2.24(N-(C*H*$_3$)$_2$), 2.28(N-C*H*$_2$-), 1.3-1.8(O-CH$_2$-(C*H*$_2$)$_4$).

Procedure for synthesizing decyl 2-bromoacetate (4): Decanol (10 g) was dissolved in dichloromethane (55 mL). Potassium carbonate, K_2CO_3 (13.08 g) was dissolved in 60 mL of distilled water and the solution was added to the organic solution. The resulting two-phase solution was cooled to 4 °C. A solution of bromoacetyl bromide (19.13 g) in dichloromethane (55 mL) was carefully added drop wise to the cooled solution while maintaining the temperature at 4 °C for about 30 min. Then the reaction mixture was stirred at room temperature for 12 h. The aqueous solution was separated and washed with dichloromethane (2 × 25 mL). The organic solution was washed with water (2 × 50 mL) and passed over the anhydrous Na_2SO_4 and concentrated to yield a white solid quantitatively. (100% yield) ^{1}H-NMR ($CDCl_3$, 400 MHz) δ/ppm: 0.878 (t, terminal, –*CH*$_3$), 1.292 (m, –(*CH*$_2$)$_7$–), 1.535 (q, –*CH*$_2$(CH$_2$)7–,), 3.258 (t, –CONH*CH2*–), 3.874 (s, –CO*CH*$_2$Br), 6.585 (br s, amide –*NH*CO).

Procedure for synthesizing 2-bromo-*N*-decylacetamide (5):Decyl amine (10 g) was dissolved in dichloromethane (55 mL). Potassium carbonate, K_2CO_3 (13.17 g) was dissolved in 60 mL of distilled water and the solution was added to the organic solution. The resulting two-phase solution was cooled to 4 °C. A solution of bromoacetyl bromide (19.25 g) in dichloromethane (55 mL) was carefully added drop wise to the cooled solution while maintaining the temperature at 4 °C for about 30 min. Then the reaction mixture was stirred at room temperature for 12 h. The aqueous solution was separated and washed with dichloromethane (2 × 25 mL). The organic solution was washed with water (2 × 50 mL) and passed over the anhydrous Na_2SO_4 and concentrated to yield a white solid quantitatively. (100% yield) ^{1}H-NMR ($CDCl_3$, 400 MHz) δ/ppm: 0.878 (t, terminal, –*CH*$_3$), 1.292 (m, –(*CH*$_2$)$_7$–), 1.535 (q, –*CH*$_2$(CH$_2$)$_7$–), 3.258 (t, –CONH*CH*$_2$–), 3.874 (s, –CO*CH*$_2$Br), 6.585 (br s, amide –*NH*CO).

Procedure for synthesizing 6-(4-benzoylphenoxy)-*N*-(2-(decyloxy)-2-oxoethyl)-*N,N*-dimethylhexan-1-aminiumbromide(6):The compound **3** (1 equiv) and the compound **4**(1.5 equiv) was taken in a screw top pressure tube in dry $CHCl_3$ and stirred at 55^0C for 36 hrs. The reaction mixture volume was reduced in rotary evaporator and precipitation was done by anhydrous diethyl ether. (70% yield) ^{1}H-NMR ($CDCl_3$, 400 MHz) δ/ppm: 7.98-6.93 (m, Ar-H), 4.86 (t,-C(O)-C*H*$_2$-CH$_2$), 4.20 (s, N-*CH*$_2$-C(O)-), 4.0 (t, Ph-O-C*H*$_2$-), 3.8 (t, O-C*H*$_2$-CH$_2$-), 3.6 (s, N-(C*H*$_3$)$_2$-), 1.5-2.0 (-C*H*$_2$-C*H*$_2$-). HRMS (m/z): calculated: 524.3734; observed: 524.3131.

Procedure for synthesizing 6-(4-benzoylphenoxy)-*N*-(2-(decylamino)-2-oxoethyl)-*N,N*-dimethylhexan-1-aminium bromide (7):The compound **3** (1 equiv) and the compounds **6** (1.5 equiv) was taken in a screw top pressure tube in dry $CHCl_3$ and stirred at 75^0C for 36 hrs. The reaction mixture volume was reduced in rotary evaporator and precipitation was done by anhydrous diethyl ether.(82% yield) ^{1}H-NMR (400 MHz, $CDCl_3$) δ/ppm: 7.98-6.93 (Ar-H), 4.86 (t,-C(O)-C*H*$_2$-CH), 4.20 (s, N-C*H*$_2$-C(O)-), 4.0 (t, Ph-O-C*H*$_2$-), 3.8 (t, N-C*H*$_2$-CH$_2$-), 3.6 (s, N-(C*H*$_3$)$_2$-), 1.5-2 (-C*H*$_2$-C*H*$_2$-). HRMS(m/z): calculated: 523.3894; observed: 523.3680.

Procedure for synthesizing 2-((6-(4-benzoylphenoxy)hexyl)dimethylammonio)acetate (9): Compound **3** (1 eqv) and *tert*-butyl bromoacetate (2 eqv) was taken in a screw top pressure tube in dry $CHCl_3$ and stirred at 55 ^{0}C for 24 h. Precipitate was done by addition of anhydrous diethyl ether. The precipitate was then dispersed in 50 mL DCM and trifluoroacetic acid was added to it and left to stir for 24 h. Volume of the mixture wax reduced in rotary evaporator and precipitation was done by diethyl ether. (65% yield) ^{1}H-NMR (400 MHz, $CDCl_3$) δ/ppm: 7.820-7.798(d, Ar-H), 7.758-7.775(d, Ar-H), 7.738-7.735(d, Ar-H), 7.584-7.577(t, Ar-H), 6.965-6.931(d, Ar-H), 4.066-4.035 (t, O-C*H*$_2$), 3.641-3.619(m, N-C*H*$_2$-CH$_2$-), 3.598-3.497(m, N-*CH*$_2$-CH$_2$-), 3.389 (s, N-(*CH*$_3$)$_2$). HRMS(m/z): calculated: 383.2097; observed: 383.2110.

Procedure of coating of cottons with compounds: Commercial cotton was cut into 1 x 1 cm^2 pieces. Compounds were dissolved in Milli-Q water to obtain aqueous solutions of concentration 10 mg/mL. The cotton pieces were dipped into the aqueous solution of compounds and were taken out. These cotton pieces soaked in the compound solution were then exposed to UV irradiation of wavelength ~ 356 nm for 20 minutes. Then they were washed in chloroform

followed by acetone to remove unbounded compound, if any. The cotton pieces were dried in vacuum at 35 ^{0}C.

2.2.3 Biological Assays

2.2.3.1 *In-vitro* Antibacterial Assay

Bacteria were grown for 6 h (about 10^8 CFU/mL). The bacterial cultures were diluted to give ~ 10^5 CFU/mL in MHB and used for determining antibacterial efficacy. Some of the compounds were water soluble and some formed dispersion in water, solubilized further by heating. Stock solutions of the compounds were prepared by serial dilution of the compounds using sterilized Milli-Q water. The aqueous solutions (20 µL) of the compounds were added to the wells of 96 well plate followed by addition of 180 µL of bacterial suspension (10^5 CFU/mL). The plates were then incubated at 37 ºC for 24 h in shaker incubator. The optical density (OD) of the bacterial suspension was recorded using TECAN (Infinite series, M200 pro) Plate Reader at 600 nm. Each concentration had triplicate values and the whole experiment was repeated twice. Antibacterial efficacy was determined by taking the average of triplicate OD values for each concentration.

2.2.3.2 *In-vitro* Antibacterial Assay of Cottons

1 x 1 cm^2 cotton pieces (both coated and uncoated) were used for the experiments. Freshly prepared MRSA ATCC 33591, were grown in nutrient broth and 10^6 CFU/mL suspensions were made in MHB. 20 microlitres of it was dropped onto the cotton pieces and incubated for 2 h at 37°C. After 2 h, the cotton pieces were dragged on nutrient agar plates followed by incubation for 24 hours at 37°C. The experiment was done in triplicate.

2.2.3.3 Non-Leaching Experiment

Methicillin-resistant *S. aureus* was collected during the log phase and 100 µL of their suspension in the media broth were plated on agar (30 mL per plate) with a wet cotton swab. Cotton pieces coated with compounds **6**, **7** as well as uncoated cotton (used as negative control) were put on the surface of the agar plates with bacteria and incubated at 37 °C for the next 24 h.

2.2.3.4 Bactericidal Kinetics of Coated Cotton

1 x 1 cm^2 cotton pieces (coated with compounds **6**, **7** and uncoated) were used for the experiments. Freshly prepared MRSA ATCC 33591 was grown in nutrient broth and 10^6 CFU/mL suspensions was made in MHB. 20 microlitres of it was dropped onto the cotton pieces and incubated for 2 h at 37 ^{0}C. After 2 h, the cotton pieces were dragged on nutrient agar plates followed by incubation for 24 hours at 37°C. The experiment was done in triplicate.

2.2.3.5 Bacterial Adhesion Test

1 x 1 cm^2 cotton pieces (coated with compound **9** and uncoated) were used for the experiments. Freshly prepared MRSA ATCC 33591 was grown in nutrient broth and 10^6 CFU/mL suspensions was made in saline. Cotton pieces were dipped in 500 µL of bacterial suspension and incubated for 2 h at 37 ^{0}C. After 2 h, the cotton pieces were dragged on nutrient agar plates followed by incubation for 24 hours at 37^0 C. The experiment was done in triplicate.

2.3 Results and Discussion

In order to estimate the antibacterial efficacy of the cationic benzophenone derivatives, their Minimum Inhibitory Concentration (MIC) was determined (Table 2.1) against different Gram-positive and Gram-negative bacteria including drug resistant bacteria and clinical isolates.

The benzophenone derivatives with non-degradable alkyl chain showed potent activity against various Gram-positive pathogens. Against *S. aureus*, the compounds showed MIC values in the range of 0.25-4 µg/mL. Against *E. faecium*, another threatening Gram-positive pathogen, the MIC values vary from 0.25-16 µg/mL; **2c** (decyl) and **2d** (dodecyl) showed MIC value of 0.25 µg/mL and 2 µg/mL against *E. faecium*. But current medical scenario is more concerned about the resistant strains and the clinically circulating strains of pathogens. All the non-degradable analogues showed highly potent activity against drug resistant Methicillin-resistant *S. aureus* (MRSA), VRE and clinically isolated strain MRSA R3889. Against both MRSA and VRE, the MIC values of **2a**-**2f** were in the range of 0.5-16 µg/mL. On checking activity against a clinically isolated strain of MRSA, R3889, MIC values varied from 0.25-2 µg/mL, proving their efficacy against various clinically relevant strains.

Table 2.1: Antibacterial activity of the benzophenone derivatives

Compounds	Minimum Inhibitory Concentration (μg/mL)								
	S. aureus	MRSA	MRSA R3889	VRE	*E. faecium*	*E. coli*	*A. baumannii*	*K. pneumoniae*	*P. aureginosa*
2a	4	16	2	16	8	32	64	256	256
2b	0.5	2	1	1	4	8	32	64	128
2c	0.25	0.5	0.25	0.5	0.25	2	32	64	128
2d	0.5	1	1	2	2	8	32	>256	>256
2e	0.5	1	1	2	16	>256	>256	>256	>256
2f	2	2	4	8	16	>256	>256	>256	>256
6	0.5	1	1	1	>256	4	>256	256	>256
7	0.5	0.5	0.5	1	>256	8	256	256	128

Compounds **2c** and **2d** showed MIC value of 0.25 μg/mL and 1 μg/mL against MRSA (R3889) respectively. On lowering or increasing the hydrophobic content by decreasing or increasing the chain length, the MIC value of the compounds obtained a higher value from an optimum value showing a parabolic trend in their activity. The compounds **2b**-**2d,** i.e. the octyl, decyl, and dodecyl analogues showed MIC in the range of 2-8 μg/mL against Gram-negative pathogen *E. coli*. On increasing the hydrophobic aliphatic chain length, activity against Gram-negative pathogens was diminished showing an increased MIC value of ≥32 μg/mL. However, the non-degradable cationic derivatives showed no potent activity against other Gram-negative pathogens including *K. pneumoniae*, *A. baumannii*, *P. aureginosa*. The degradable analogues, **6** (ester) and **7**(amide) showed excellent efficiency against the tested Gram-positive pathogens (excluding *E. faecium*) including drug-resistant and clinically isolated strains. Their MIC values varied in the range of 0.5-1 μg/mL against *S. aureus*, MRSA (R3889) and VRE. Compounds **6** and **7** were active against *E. coli* having MIC values 4 μg/mL and 8 μg/mL respectively, but MIC values against other Gram-negative pathogens were much higher (≥ 128 μg/mL).Compounds **6** and **7** were selected for coating on cotton textile.

Unbleached cotton was bought from local commercial market. Cotton was washed with isopropanol and cut into 1 x 1 cm^2 pieces which were further washed with acetone to remove impurities, if any. These cotton pieces were coated by dipping them into aqueous solutions of the compounds **6** and **7** of concentration 10 mg/mL. After 10 mins of UV irradiation, the cotton pieces were turned onto the other side and UV was exposed for 10 more minutes.

The coated cottons were tested for their antibacterial activity against various Gram-positive pathogens including drug-resistant and clinically isolated strains. Uncoated cottons were used as negative controls to check whether they themselves have any antibacterial activity or not. Upon incubation with 20 µL of 10^6 CFU/mL of bacteria for 24 h, a lawn of bacteria was seen in the agar plate for uncoated cottons, showing their inefficacy to kill bacteria.

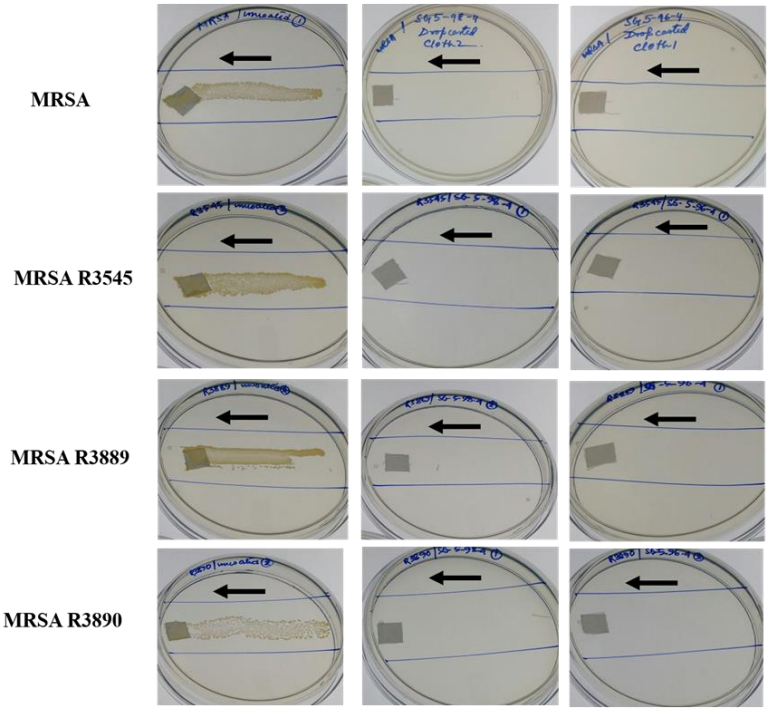

Figure 2.1: Activity of A) uncoated cottons, B) cottons coated with compound **6**, C) cottons coated with compound **7** against various Gram-positive pathogens.

On the other hand, no bacterial growth was observed in the agar plate for the cottons coated with compounds **6** and **7** respectively (Figure 2.1). The coated cottons not only killed

MRSA, but also showed no growth for the clinically isolated strains MRSA (R3545, R 3889, and R3890). Coated ones also showed complete inhibition of growth of *E. faecium* and VRE.

As discussed earlier in the introduction, benzophenone was employed in the molecular structure for covalent linking of the molecules to the textile surface. This imparted a permanent coating to the cotton. To check whether the compounds were leaching out from the surface and killing bacteria in the surroundings, the coated cotton pieces were tested to observe zone of inhibition of bacterial growth, if any. Cottons pieces were placed on agar plates with bacteria spread on the agar. Uncoated cottons were also used in the experiment as negative controls. Upon incubation, neither the coated nor the uncoated cottons showed any zone of inhibition around them. In enlarged images it can be observed that there is no inhibition of bacterial growth surrounding the cotton pieces (Figure 2.2). This emphasizes on the fact that there was no leaching of compound from the coated cottons.

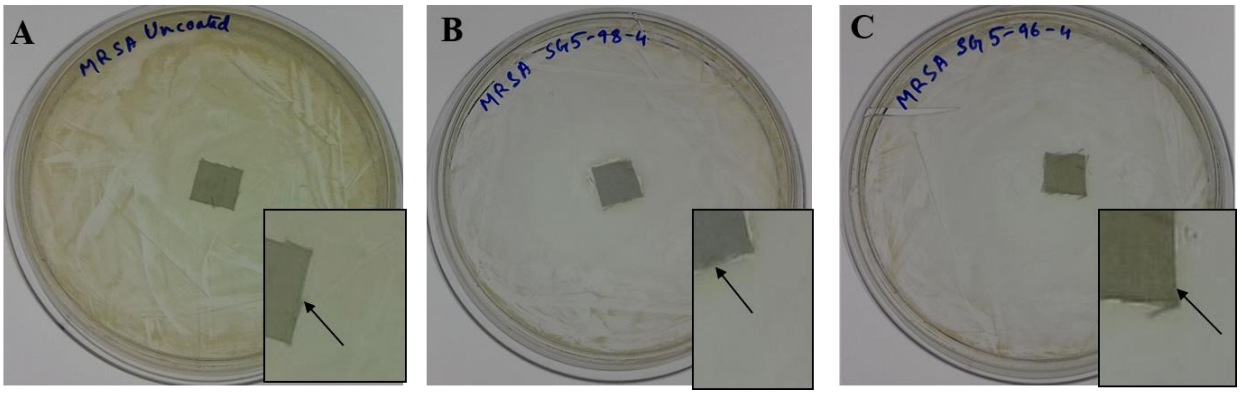

Figure 2.2: Non-leaching of A) uncoated cottons; cottons coated with B) compound **6** and C) compound **7** respectively.

Bacterial colonization by nosocomial pathogens on material surfaces can cause serious and life-threatening infections. Textiles are being used on a regular basis, and are most prone to be contaminated by common infection spreading mechanisms, such as coughing, sneezing etc. Hence, textile surfaces are one of the most exposed material that can get infected and transmit the infection. Therefore, the modified textile surfaces need to kill the microbes in a rapid manner. To evaluate how fast the textile surfaces can kill bacteria, time-kill kinetics experiment was performed. Upon incubation with MRSA, cotton surfaces coated with compound **6** killed

bacteria completely in 30 minutes, whereas cotton surfaces coated with compound **7** showed complete killing in 1 h (Figure 2.3).

Biomaterial surfaces not only need to be antibacterial, but also need to release the dead bacterial cells preventing their accumulation on the surface. This "kill−release" strategy has been applied to construct so-called smart antibacterial surfaces, which can kill bacteria attached to their surface and then undergo release of the dead bacteria and other debris. Several groups have developed surfaces grafted with zwitterionic polymers that strongly bind water molecules via electrostatic interactions to form a stable hydration layer in aqueous solution and show excellent non-fouling properties. Compounds **6** and **7** upon degradation, will give the zwitterionic compound **9**. The textiles coated with compounds **6** and **7** which were initially antibacterial, would switch to antifouling surfaces, as a result of degradation of the compounds on the surfaces.

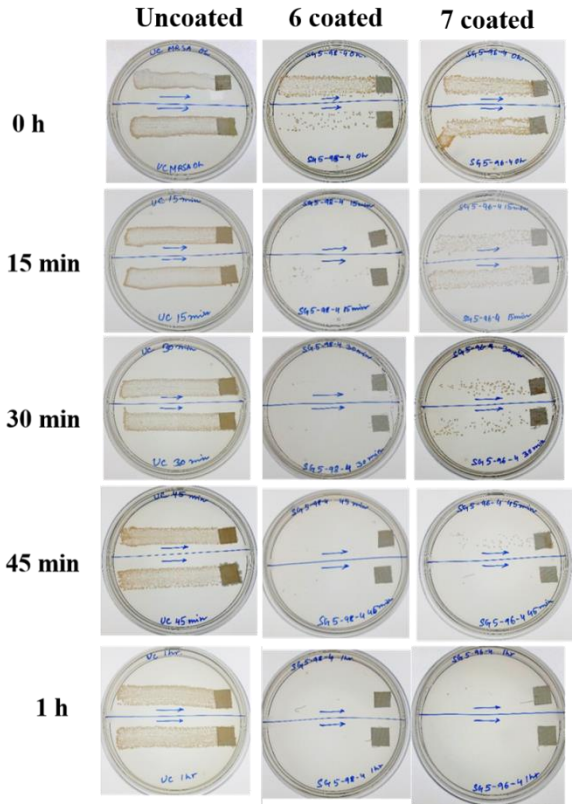

Figure 2.3: Bactericidal killing kinetics of uncoated cottons and cotton textile coated with compounds **6** and **7**.

To check whether textile surfaces exert any antifouling effect, cotton pieces were coated with compound **9** and tested for bacterial adhesion when kept immersed in a bacterial suspension. Cotton pieces coated with compound **9** showed much less adherence of bacteria compared to the uncoated ones. To eliminate the possibility of bacterial killing by compound **9**, its antibacterial activity was checked and was found to be inactive. Hence the inhibited growth of bacteria in the plate (Figure 2.4) was due to lower adherence of bacteria to the textile surface coated with the zwitterionic compound **9**.

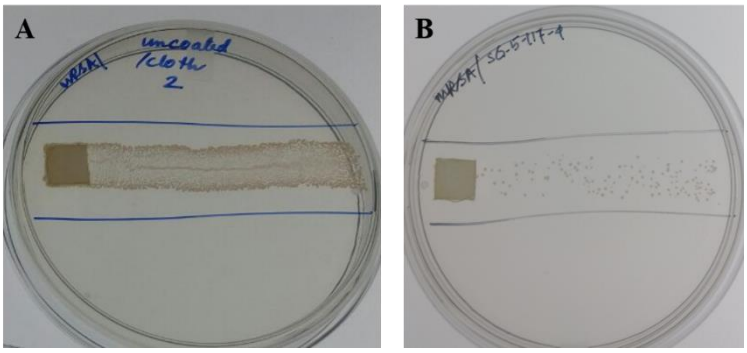

Figure 2.4: Bacterial adhesion to A) uncoated cottons and b) cotton coated with compound **9**

2.4 Conclusion

In conclusion, a series of cationic benzophenone derivatives have been prepared. Compounds **6** and **7** were coated on cotton textile from their aqueous solutions. The coated cottons showed excellent activity against various Gram-positive bacteria including drug resistant and clinically isolated strains. Cottons were coated with the zwitterionic compound **9** which is the degradation product of the compounds **6** and **7**. These showed lower adherence of bacterial cells to the cotton surface owing to its antifouling nature. This switchable permanent coating has potential for various applications.

References

(1) Kenawy, E.-R.; Worley, S. D.; Broughton, R. *Biomacromolecules* **2007**, *8*, 1359.

(2) Patel, M. B.; Patel, S. A.; Ray, A.; Patel, R. M. *J. Appl. Polym. Sci.* **2003**, *89*, 895.

(3) Ferreira, L.; Zumbuehl, A. *J. Mater. Chem.* **2009**, *9*, 7796.

(4) Gabriel, G. J.; Som, A.; Madkour, A. E.; Eren, T.; Tew, G. N. *Mater. Sci. Eng.*, **2007**, *57*, 28.

(5) Klibanov, A. M. *J. Mater. Chem.* **2007**,*17*, 2479.

(6) Ferreira, L.; Zumbuehl, A. *J. Mater. Chem.* **2009**, *19*, 7796.

(7) Wach, J. Y.; Bonazzi, S.; Gademann, K. *Angew. Chem. Int. Ed. Engl.* **2008**, *47*, 7123.

(8) Pritchard, E. M.; Valentin, T.; Panilaitis, B.; Omenetto, F.; Kaplan, D. L. *Adv. Funct. Mater.* **2013**, *23*, 854.

(9) Cado, G.; Aslam, R.; Seon, L.; Garnier, T.; Fabre, R.; Parat, A.; Chassepot, A.; Voegel, J. C.; Senger, B.; Schneider, F.; Frere, Y.; Jierry, L.; Schaaf, P.; Kerdjoudj, H.; Metz-Boutigue, M. H.; Boulmedais, F. *Adv. Funct. Mater.* **2013**, *23*, 4801.

(10) Lin, J.; Qiu, S.; Lewis, K.; Klibanov, A. M. *Biotechnol. Prog.* **2002**,*18*,1082.

(11) Lin, J.; Qiu, S.; Lewis, K.; Klibanov, A. M. *Biotechnol. Bioeng.* **2003**, *83*, 168.

(12) Lin, J.; Murthy, S. K.; Olsen, B. D.; Gleason, K. K.; Klibanov, A. M. *Biotechnol. Lett.* **2003**, *25*, 1661.

(13) Milović, N. M.; Wang, J.; Lewis, K.; Klibanov, A. M. *Biotechnol. Bioeng.* **2005**, *90*, 715.

(14) Park, D.; Wang, J.; Klibanov, A. M. *Biotechnol. Prog.* **2006,** *22*, 584.

(15) Haldar, J.; An, D.; Alvarez de Cienfuegos, L.; Chen, J.; Klibanov, A. M. *Proc. Natl. Acad. Sci. U. S. A.* **2006**, *103*, 17667-17671.

(16) Haldar, J.; Chen, J.; Tumpey, T. M.; Gubareva, L. V.; Klibanov, A. M. *Biotechnol. Lett.* **2008**, *30*, 475.

(17) Haldar, J.; Weight, A. K.; Klibanov, A. M. *Nat. Protoc.* **2007**, *2*, 2412.

(18) Larson, A. M.; Hsu, B. B.; Rautaray, D.; Haldar, J.; Chen, J.; Klibanov, A. M. *Biotechnol. Bioeng.* **2011**, *108*, 720.

(19) Tiller, J. C.; Liao, C. J.; Lewis, K.; Klibanov A. M. *Proc. Natl. Acad. Sci.* **2001**, *98*, 5981.

(20) Lee, S. B.; Koepsel, R. R.; Morley, S. W.; Matyjaszewski, K.; Sun, Y.; Russell, A. J. *Biomacromolecules* **2004**, *5*, 877.

(21) Dorman, G.; Prestwich, G. D. Biochemistry **1994**, *33*, 5661.

(22) Swan, D. G.; Amos, R. A.; Everson, T. P. U.S. Patent US6077698, **2000**.

(23) Prestwich, G.; Dorman, G.; Elliott, J.; Marecak, D.; Chaudhary,´ A. *Photochem. Photobiol.* **1997**, *65*, 222.

(24) Turro, N. J. Modern Molecular Photochemistry; Benjamin/ Cummings: Menlo Park, CA, **1978**.

(25) Lin, A. A.; Sastri, V. R.; Tesoro, G.; Reiser, A.; Eachus, R. *Macromolecules* **1988**, *21*, 1165.

(26) McCaig, M. S.; Paul, D. R. *Polymer* **1999**, *40*, 7209.

(27) Oster, G.; Oster, G. K.; Moroson, H. *J. Polym. Sci.* **1959**, 671.

(28) Lin, A. A.; Sastri, V. R.; Tesoro, G.; Reiser, A.; Eachus, R. *Macromolecules* **1988**, *21*, 1165.

(29) Brauchle, C.; Burland, D. M.; Bjorklund, G. C. *J. Phys. Chem.* **1981**, *85*, 123.

(30) Higuchi, H.; Yamashita, T.; Horie, K.; Mita, I. *Chem. Mater.* **1991**, *3*, 188.

(31) Turro, N. J. Modern Molecular Photochemistry; University Science Books: Mill Valley, CA, **1991**.

(32) Wong, S. Y.; Moskowitz, J. S.; Veselinovic, J.; Rosario, R. A.; Timachova, K.; Blaisse, M. R.; Fuller, R. C.; Klibanov, A. M.; Hammond, P. T. *J. Am. Chem. Soc* **2010,** *132*, 17840.

(33) Han, H.; Wu, J. F.; Avery, C. W.; Mizutani, M.; Jiang, X. M.; Kamigaito, M.; Chen, Z.; Xi, C. W.; Kuroda, K. *Langmuir* **2011,** *27*, 4010-4019.

Chapter 3

Hydroxyapatite Loaded with Quaternary Chitosan-Silver Chloride Nanocomposites Selectively Kill Bacteria over Human Erythrocytes

Abstract

This chapter reports the *in-situ* synthesis of highly effective dual-action polymer-silver chloride nanocomposites from an aqueous solution of a quaternary chitosan derivative and a silver salt. The cationic water-soluble antimicrobial polymers acted as both reducing and stabilizing agents to the silver chloride nanoparticles. The polymeric nanocomposites were shown to be effective against both Gram-positive and Gram-negative bacteria including the drug-resistant pathogens such as methicillin-resistant *S. aureus* (MRSA), beta lactam-resistant *K. pneumoniae* and various clinically isolated strains. The most active nanocomposite **QAm_1-Ag_1** showed highly potent activity against Gram-negative pathogens (MIC in the range of 8-32 µg/mL), whereas the polymer alone was shown to be inactive against them. The nanocomposite killed *E. coli* (~5 log reduction) in 30 minutes. Further, the composite **QAm_1-Ag_1** was loaded with hydroxyapatite (**HAp**). Disks formed from the loaded **HAp** were shown to be effective in inhibiting bacterial growth. Notably, negligible *in-vitro* toxicity towards human erythrocytes was observed for both **QAm_1-Ag_1** and the composite-loaded hydroxyapatite (**HAp/QAm_1-Ag_1**). Hydroxyapatite loaded with quaternary polymeric nanocomposite **QAm_1-Ag_1** thus could be used as safe and effective antimicrobial biomaterial device in orthopaedic applications.

3.1 Introduction

Despite sterilization and aseptic procedures, bacterial infection remains a major threat to the usage of medical implants.[1] Systemic administration of antibiotics is costly and shows lesser efficacy against implant-associated infections.[2] Thus the cases of implant removal and revision surgery are increasing which increases patients' sufferings and healthcare-cost.[1-3] Though revision surgery can remove/reduce infections, various other complications such as re-infections of the implants, due to surgical procedure or from the surrounding microbes can result.[4] Thus, development of antimicrobial materials which can not only prevent infection but also eliminate bacteria in the surroundings, is highly demanded.

Antimicrobial polymeric nanocomposites, offer great potential and several advantages over the existing individual systems.[5-8] These materials not only kill pathogen on contact but also release active antimicrobials into the surroundings thereby killing microbes in the vicinity. Moreover, the nanomaterials can release the active antimicrobials over an extended period providing long-lasting antibacterial activity particularly required to eliminate device-related infections.

Orthopaedic devices are the most common surgical devices associated with implant-related infections. The gold standard biomaterial for local antibiotic delivery against bone-infections, poly(methyl methacrylate) (PMMA) bone cement, bears many limitations. Such shortcomings include limited antibiotic release, incompatibility with many antimicrobial agents, and the need for follow-up surgeries to remove the non-biodegradable cement before surgical reconstruction of the lost bone.[9,10] Hydroxyapatite-based products were first introduced in ceramic form and have raised much interest because they are chemically integral to the skeletal system.[11-13] Hydroxyapatite was later introduced in granular and paste forms, which were more osteoconductive, much more easily shaped, and did not create an inflammatory response.[14]

Among various nanoparticles, silver-based nanoparticles are of special interest because of their broad-spectrum antimicrobial activity toward different pathogens, e.g., bacteria, fungi, viruses, etc.[15,16] Silver-containing materials have been widely used by the biomedical industry in catheters, dental material, medical devices, implants, and wound dressings.[17-19] However, most of

the techniques used to incorporate silver into polymeric matrices involve complex synthesis. [20-24] Also, the polymers in the nanocomposites are generally poorly antimicrobial.

Chitosan, a natural polycationic linear polysaccharide derived from chitin, has been employed in various biomedical applications. This chapter reports development of a water soluble quaternary chitosan polymer *N*-(2-hydroxy) propyl-3-trimethyl ammonium chitosan chloride (HTCC)-silver chloride nanocomposite capable of inactivating both Gram-positive and Gram-positive bacteria. The polymer-nanocomposites were shown to be non-toxic to human erythrocytes. HTCC is known to be moderately active against Gram-positive bacteria but its activity is very low against Gram-negative bacteria. The water-soluble nanocomposites were loaded on hydroxyapatite. Their activity was checked against various pathogens under in-vitro conditions. Zone of inhibition was studied to study their release-based killing. The disks formed by HAp/QAm_1-Ag_1 showed no significant toxicity towards human erythrocytes.

3.2 Experimental Section

3.2.1 Materials and Instrumentation

All the solvents were of reagent grade, which were distilled and dried before its uses. All the reagents were purchased from Sigma-Aldrich, S.D. Fine, and Spectrochem were used without further purification. Nuclear magnetic resonance spectra were recorded on Bruker (AV-400) 400 MHz spectrometer in deuterated solvents. For optical density measurement Tecan InfinitePro series M200 Microplate Reader was used. Bacterial strains, *S. aureus* (MTCC 737), *P. aureginosa* (MTCC 424) *E. coli* (MTCC 443) were purchased from MTCC (Chandigarh, India). Methicillin-resistant *S. aureus* (ATCC 33591), *Enterococcus faecium* (ATCC 19634), vancomycin-resistant *Enterococcus faecium* (ATCC 51559), and *Klebsiella pneumoniae* (ATCC 700603) were obtained from ATCC (Rockville, MD, USA).

3.2.2 Synthesis and Characterization

3.2.2.1 Reaction Scheme

Chitosan is a glucosamine derived from naturally occurring polymer chitin. HTCC, a modified quaternary chitosan was synthesized following a previous protocol (Scheme 3.1A).[25] The

quaternary group of the polymer possess chloride-counter ions. These chloride ions were employed for nanoprecipitation of AgCl nanoparticles. Free amine present in the polymer acted as a stabilizer of the nanoparticles.

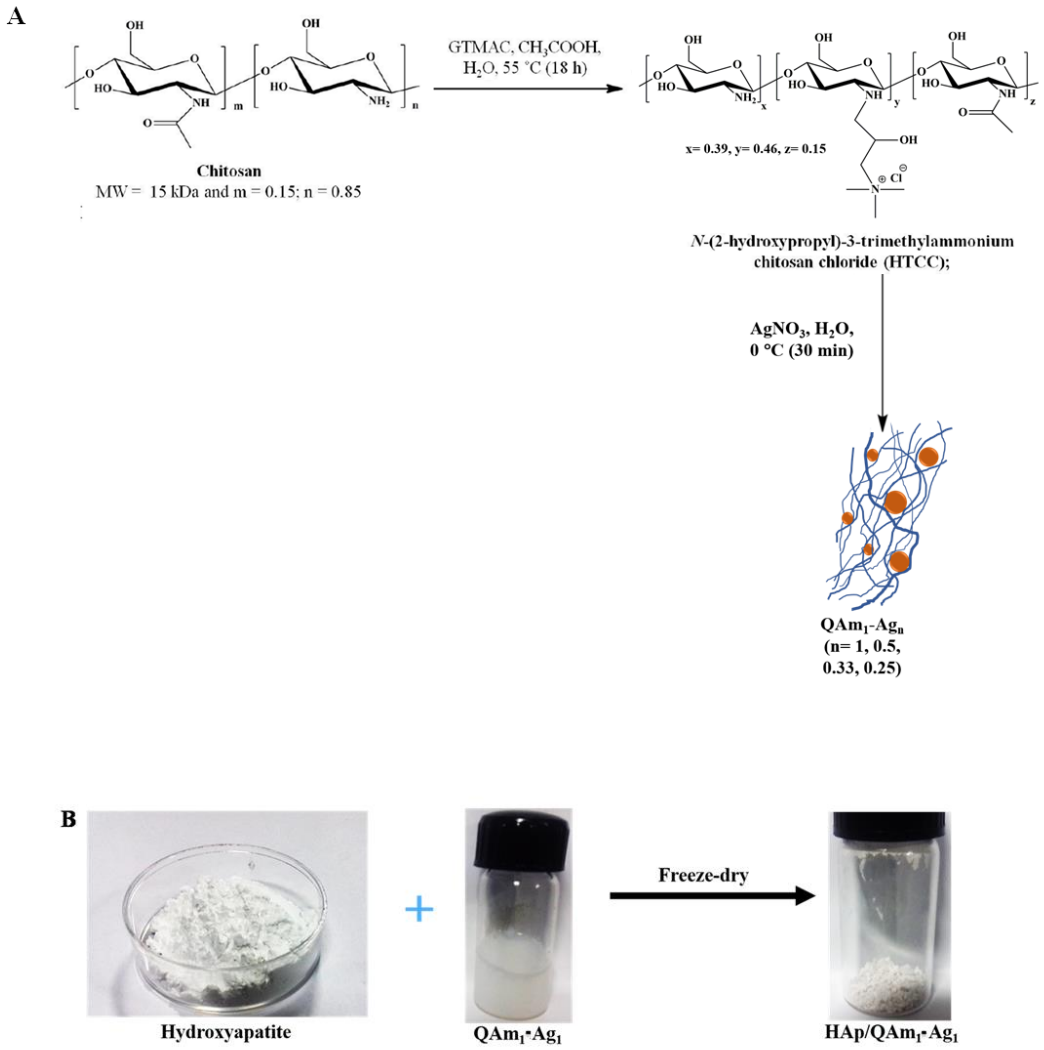

Scheme 3.1: A) Synthesis of HTCC polymer and its silver chloride nanocomposites. B) Preparation scheme of hydroxyapatite-HTCC-silver chloride nanocomposite (**HAp/QAm$_1$-Ag$_1$**).

3.2.2.2 Synthetic Protocol and Characterization

Synthesis of Quaternized Chitosan Derivatives (HTCC): Chitosan (2.5 g) was suspended in Millipore water (200 mL), and then acetic acid (1 mL, 0.5%, v/v) was added to the suspension. The chitosan-acetic acid mixture was stirred for about 12 h at room temperature to obtain a clear

solution. Glycidyl trimethylammonium chloride (GTMAC) was then added to the polymer solution in three portions at nearly 2 h intervals. The GTMAC to chitosan mole ratio was 8:1. The reaction was allowed to proceed at 55 ˚C for 18 h after the final addition of GTMAC. The reaction mixture was then diluted with 300 mL water and the product was precipitated with excess of acetone. The chitosan derivatives were filtered through a sintered glass funnel and washed with acetone repeatedly and finally with acetone-ethanol mixture (1:1). The products were characterized by ^{1}H NMR and FT-IR spectroscopy (yield higher than 90%). FT-IR (ATR): υ = 3445−3162 cm^{-1} (−OH and $-NH_2$ or −NH−), 1682 cm^{-1} (amide I, C=O str.), 1555 cm^{-1} (amide II, NH ben.), 1478 cm^{-1} ($-N^{+}(CH_3)_3$ ben.). 1H NMR ($CDCl_3$, 400 MHz,) δ/ppm: 1.910 (s, $-CH_3COO-$), 2.068 (s, $-CH_3CO-$), 2.568−2.939 (m, $-NHCH_2CH(OH)CH_2-$ and Cell C2H), 3.228 (s, $-CH(OH)CH_2N^{+}(CH_3)_3$), 3.412− 3.991 (m, Cell C3H−C5H, $-CH(OH)CH_2N^{+}(CH_3)_3$), 4.292 (s, $-CH_2CH(OH)CH_2-$), 4.546 (s, Cell C1H).

Determination of Degree of Substitution (DS): The degree of substitution (DS) or degrees of quaternization (DQ) in the quaternary chitosan derivative was determined by conductivity measurement. DS was calculated by titrating the amount of chloride (Cl^{-}) ions on the polymer with aqueous $AgNO_3$ solution. The moles of reacted GTMAC to the moles of repeating sugar unit of chitosan was defined as DS. **HTCC** polymer (0.025 g) was dissolved in Millipore water (50 mL) and then solution of $AgNO_3$ (0.02 M) was used to titrate the polymer solution. The DS of **HTCC** polymer was calculated using the following equation:

$$C_{AgNO3} \times V_{AgNO3} = (m_{HTCC} \times DS)/ [(DS \times M_3) + \{(1-DS-DA) \times M_1\} + (DA \times M_2)]$$

In this equation, C_{AgNO3} is the concentration of $AgNO_3$, V_{AgNO3} is the volume of the $AgNO_3$ solution at the point of equivalence, m_{HTCC} is the mass of **HTCC** used for titration, M_1 is the molecular weight of the glucosamine repeating unit, M_2 is the molecular weight of the N-acetyl glucosamine repeating unit, M_3 is the molecular weight of GTMAC substituted repeating unit, i.e., quaternary unit, DA is the degree of acetylation of the native chitosan (0.15).

Synthesis of Quaternary Chitosan-Silver Chloride Nanocomposites: On measurement of the DS of **HTCC**, the number of moles of the quaternary unit in the polymer was calculated. 1 g HTCC was dissolved in Millipore water. Aqueous solutions of $AgNO_3$ were prepared with required equivalents of $AgNO_3$ such that quaternary unit (QAm) and Ag^{+} ions had a molar ratio 1:1, 1:0.5,

1:0.33 and 1:0.25. The $AgNO_3$ solutions were added drop-wise to polymer solution at 0 ˚C with vigorous stirring. After 2 h, the mixtures were freeze-dried and stored in dark.

Characterization of nanocomposites: To monitor the growth of the silver nanoparticle, the reaction mixture was directly used for UV-visible absorption spectroscopy. 20 μL of the reaction mixture was taken in 1.980 mL of Millipore water in cuvettes with water as a blank. Spectra were recorded for the region 150-800 nm. For TEM imaging, solid composites were re-dissolved in Millipore water and then drop casted on TEM grid. After casting onto the grids, they were allowed for drying and were stored in vacuum desiccator. Solid samples were directly used for X-ray diffraction spectra.

Synthesis of Nanocomposite-Loaded Hydroxyapatite: QAm_1-Ag_1 was dissolved in water making an aqueous solution of 16.6 mg/mL. 2 gm of **HAp** was mixed with 6 mL of the aqueous solution of **QAm_1-Ag_1**. Upon freeze-drying this mixture, white powder was obtained which was pulverized and used for further experiments.

Characterization of hydroxyapatite loaded with nanocomposite: Hydroxyapatite loaded with nanocomposite (**HAp/QAm_1-Ag_1**) was characterized by UV/Vis spectrum taking aqueous dispersion of the sample. The solid sample was re-dispersed in Millipore water and spectra were recorded as discussed earlier. UV/Vis spectrum for **HAp** was also recorded as a control.

3.2.3 Biological Assays

3.2.3.1 *In-vitro* Antibacterial Assay

The same protocol was followed as described in the section of 2.2.3.1 in Chapter 2.

3.2.3.2 Haemolytic Assay

Studies on human subjects were performed according to the guidelines approved by Institutional Bio-Safety Committee (IBSC) at Jawaharlal Nehru Centre for Advanced Scientific Research (JNCASR). Blood was donated by a healthy human donor and red blood cells (RBCs) were isolated from the heparinised blood. The cells were then washed twice and finally resuspended in PBS (5 vol%). Cell suspension (150 μL) was then added to solutions of serially diluted compounds taken in the wells of a 96-well plate (50 μL). Two controls were prepared, one without the compounds

(only 50 µL water) and the other with 0.1 vol% solution of Triton X-100 (TX, 50 µL). The plate was then incubated at 37 °C for 1 h. Next, cells were centrifuged at 3500 rpm for 5 minutes. Supernatants from the wells (~100 µL) were then transferred to a new 96-well plate and absorbances of the supernatants were recorded at 540 nm. Percentage of hemolysis was calculated as $(A–A_o)/(A_{total}–A_o) \times 100$, where A is the absorbance for the test samples, A_o is the absorbance for the wells contained only water and RBC suspension, and A_{total} the absorbance of fully lysed cells (wells with TX), all at 540 nm.

3.2.3.3 Bactericidal Kinetics

The bactericidal activity of the compounds was evaluated by performing time kill kinetics assay. This gives the information about the rate at which the compounds are acting on bacteria. Briefly, *S. aureus* and *E. coli* was grown in nutrient broth at 37 ºC for 6 h. The compounds **HTCC** and **QAm$_1$-Ag$_1$** were added to the bacterial solution (*S. aureus* of approximately 1×10^5 CFU/mL and *E. coli* of approximately 8.5×10^5 CFU/mL) with the working concentration of 192 µg/mL against *S. aureus* and 96 µg/mL against *E. coli*. This was incubated at 37°C. At different time intervals (15 min, 30 min, 45 min, 60 min, 90 min and 120 min against *S. aureus* and 10, 20, 30, 40, 50, 60 min against *E. coli*) 20 µL of aliquots from that solution were serially diluted 10-fold in 0.9 % saline. Then from the dilutions, 20 µL was plated on nutrient agar plates and incubated at 37 ºC for 24 h. The bacterial colonies were counted and results are represented in logarithmic scale, i.e. $\log_{10}$ (CFU/mL).

3.2.3.4 Zone of Inhibition

E. coli and Methicillin-resistant *S. aureus* were collected during the log phase and 100 µL of their suspension in the media broth was plated on agar (30 mL per plate) with a wet cotton swab. **HAp/QAm$_1$-Ag$_1$** and **HAp** composites were compacted into 200-mg discs. The discs were manufactured by direct compressing of the powders using 8 mm stainless steel die by hand-pressing. Disks of **HAp/QAm$_1$-Ag$_1$** composites and **HAp** (used as negative control) were put on the surface of the agar plates with bacteria and incubated at 37 °C for the next 24 h. The zones of inhibition of bacteria growth were photographed. The test was performed in duplicate.

3.2.3.5 Toxicity of Hydroxyapatite Discs to Red Blood Cells

Blood was donated by a healthy human donor and red blood cells (RBCs) were isolated from the heparinised blood. The cells were then washed twice and finally resuspended in PBS (5 vol%). 50 µL of cell suspension was dropped on 8 mm disks of **HAp** and **HAp/QAm$_1$-Ag$_1$** disks prepared as discussed previously. Incubation was done at 37 °C for 1 h and images were recorded.

3.3 Results and Discussion

Chitosan, a natural glucosamine polymer, has *N*-acetyl (15%) and free amine (85%) groups. It was modified by reacting with glycidyl trimethylammonium chloride, which introduces a quaternary ammine group into the polymeric structure with chloride as counter ions. The degree of substitution, i.e. DS was calculated by titration of the chloride ions with an aqueous solution of $AgNO_3$. Upon titration, the degree of substitution was found to be ~53% of the free amine groups present in the polymeric architecture. Therefore in the final polymer contents 39% free amine, 46% of the quaternary group and 15% of *N*-acetyl bearing sugar units (Scheme 3.1A).

The presence of chloride ions made this quaternary polymer suitable for *in-situ* synthesis of silver chloride nanoparticles by nanoprecipitation (Scheme 3.1A). The polymer nanocomposites were prepared by adding aqueous solution of silver nitrate ($AgNO_3$) to an aqueous solution of the polymer under dark condition. Four different composites were prepared by varying the molar ratio of the quaternary amine group (QAm) of the polymer and silver ions (Ag^+) as 1:1 (QAm_1-Ag_1), 1:0.5 (QAm_1-$Ag_{0.5}$), 1:0.33 (QAm_1-$Ag_{0.33}$) and 1:0.25 (QAm_1-$Ag_{0.25}$). The formation of silver chloride nanoparticles was indicated by the appearance of opaque white colour with time. The solid polymer-AgCl nanocomposites were obtained by rapid dialysis and freeze drying of the nanocomposite solutions.

UV/Visible spectra were recorded for the polymer nanocomposites which showed maxima at around 269 nm, which corresponds to the surface plasmon resonance band of silver chloride nanoparticles (Figure 3.1A). This maximum was absent in case of **HTCC**. To establish that the nanoparticles were those of AgCl and not of some other species such as any metallic oxide or metallic silver, XRD spectra of the nanocomposites were recorded. For all the four nanocomposites, peaks were found at 2θ values 27.8°, 32.3°, 46.4°, 54.8°, 57.5°, 67.5°, 76.8°, 85.6° (Figure 3.1B) which corresponds to the planes 111, 200, 220, 311, 222, 400, 420, 422.

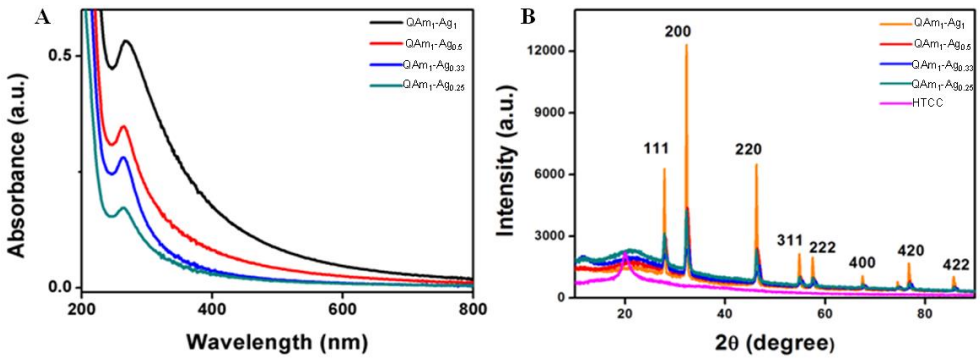

Figure 3.1 Characterization of Nanocomposite. A) UV/Vis spectra of polymer nanocomposites. B) X-ray diffraction spectra of **HTCC** and nanocomposites.

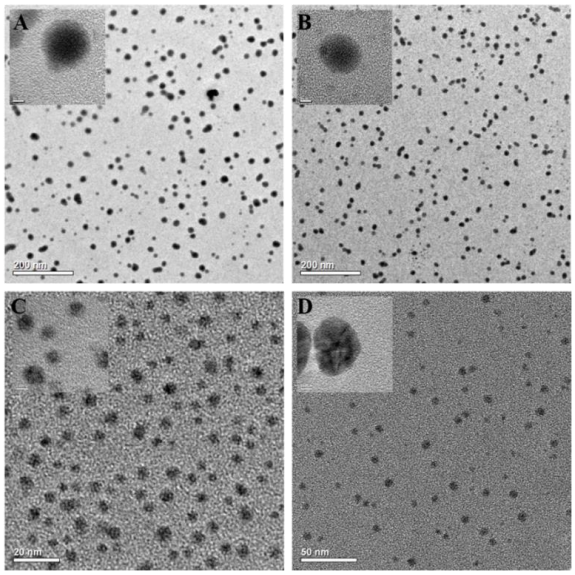

Figure 3.2: Characterization of nanoparticle-dimensions by TEM. A) **QAm$_1$-Ag$_1$**, B) **QAm$_1$-Ag$_{0.5}$**, C) **QAm$_1$-Ag$_{0.33}$** and D) **QAm$_1$-Ag$_{0.25}$**.

The size of nanoparticles and their distribution play a significant role in determining their activity. To investigate the dimension of the polymer-capped nanoparticles, TEM images were

recorded which showed that the nanoparticles had a size distribution ranging between 10-40 nm. The nanocomposites with lower silver content were found to have more of smaller nanoparticles owing to the higher number of capping agents available (Figure 3.2).

The antibacterial efficacy of the polymeric nanocomposites was evaluated by challenging them against a wide spectrum of drug sensitive and drug resistant bacteria such as *S. aureus*, *E. coli*, *P. aeruginosa*, *A. baumannii* and drug resistant bacteria such as MRSA, VRE. The antibacterial efficacy was expressed as minimum inhibitory concentration (MIC), i.e., the minimum concentration of the composites required to inhibit the growth of bacteria. Antibacterial efficacy of the polymer was also evaluated to compare the results against the same bacteria (Table 3.1). The polymer **HTCC** showed moderate activity against Gram-positive bacteria (32-128 µg/mL) but activity against Gram-negative bacteria was very low (≥256 µg/mL). Against various Gram-positive pathogens, all the nanocomposites and **HTCC** were

Table 3.1: Antibacterial efficacy and haemolytic activity of polymer-nanocomposites

Compounds	MIC (Minimum Inhibitory Concentration) (µg/mL)										HC_{50} (µg/mL)
	S. aureus	MRSA	MRSA R 3545	MRSA R 3889	MRSA R 3890	*E. faecium*	*E. coli*	*A. baumannii*	*K. pneumoniae*	*P. aureginosa*	
QAm_1-Ag_1	32	16	16	32	32	128	16	8	32	16	> 1024
QAm_1-$Ag_{0.5}$	32	32	16	32	32	256	32	16	64	32	> 1024
QAm_1-$Ag_{0.33}$	32	32	16	32	32	256	32	32	64	32	> 1024
QAm_1-$Ag_{0.25}$	32	32	16	32	32	256	32	32	64	32	> 1024
HTCC	128	128	32	128	128	>256	256	256	>256	256	> 1024

active. Against *S. aureus*, all the nanocomposites showed MIC values 32 µg/mL whereas that of **HTCC** MIC 128 µg/mL. Against MRSA, MIC values of the nanocomposites ranged from 16-32 µg/mL. The nanocomposites showed MIC values in the range of 16-32 µg/mL against the clinically isolated strains of MRSA. Against *E. faecium*, **QAm_1-Ag_1** showed MIC of 128 µg/mL whereas that of **HTCC** was found to be >256 µg/mL. Their activity was checked against various Gram-negative pathogens, such as *E. coli*, *A. baumannii*, *K. pneumoniae*, and *P. aureginosa*.

Among all four nanocomposites, **QAm_1-Ag_1** showed higher activity than the other composites. This can be validated by the fact that **QAm_1-Ag_1** had highest content of silver chloride nanoparticles. Against *E. coli*, the nanocomposites showed MIC values in the range 16-32 µg/mL; **QAm_1-Ag_1** having MIC value 16 µg/mL. This proved their potential of inactivating microbes, especially Gram-negative ones, much higher compared to the polymer alone. The composites were also much potent compared to **HTCC** against *A. baumannii*, the most dangerous pathogen according to the priority pathogen list published by WHO in 2017. MIC value of **QAm_1-Ag_1** against *A. baumannii* was 8 µg/mL and that of only polymer **HTCC** was 256 µg/mL. Against the other two Gram-negative pathogens *K. pneumoniae* and *P. aureginosa*, the MIC values of the nanocomposites were in the range of 16-64 µg/mL whereas **HTCC** had MIC value of 256 µg/mL against these two pathogens. Among the four nanocomposites, **QAm_1-Ag_1** was shown to be the most active one with MIC values ranging between 16-128 µg/mL against tested Gram-positive pathogens and 8-32 µg/mL against Gram-negative ones.

Silver is known to have cytotoxic effects. To check the toxicity of the nanocomposites to human red blood cells (RBCs), their HC_{50} values were determined. HC_{50} value is the concentration of the compound which lyse 50% of human RBCs. Incorporation of silver chloride nanoparticles into the polymer did not introduce much toxicity as all the nanocomposites had HC_{50} values >1024 µg/mL. The HC_{50} value of **HTCC** was also found to be >1024 µg/mL.

To check how fast the nanocomposite could kill bacteria, bactericidal kinetics of **QAm_1-Ag_1** was checked against *S. aureus* and *E. coli*. Against *S. aureus*, at 192 µg/mL, **QAm_1-Ag_1** showed only 1.5-log reduction in bacterial number in 2 hours whereas **HTCC** showed 1 log reduction in the same time (Figure 3.3A). Against *E. coli*, at 96 µg/mL, **QAm_1-Ag_1** showed complete killing of bacteria (~ 5 log reduction) in only 30 minutes, whereas **HTCC** showed no significant reduction in bacterial count (Figure 3.3B). This proves the high potency of **QAm_1-Ag_1** against Gram-negative bacteria due to the presence of silver chloride nanoparticles, as silver nanoparticles are known to be effective against Gram-negative pathogens.

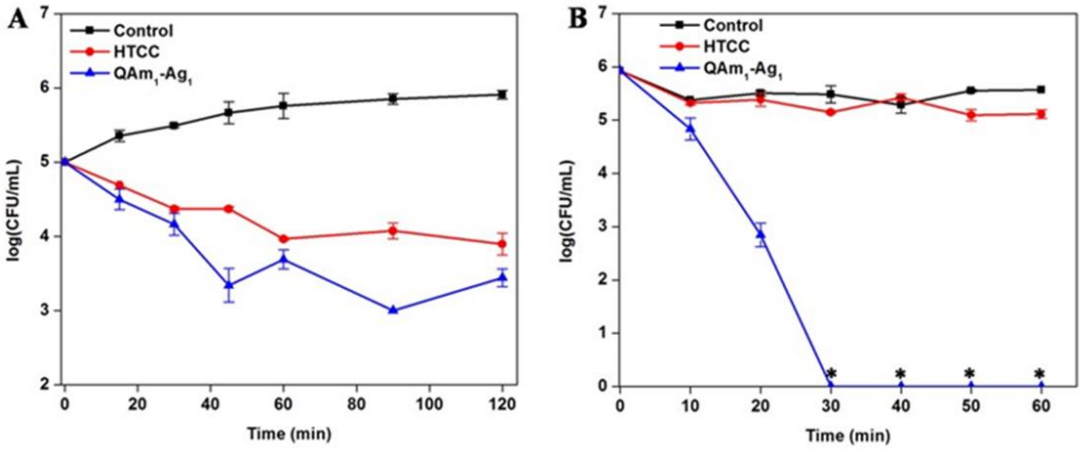

Figure 3.3: Bactericidal kinetics of **QAm$_1$-Ag$_1$** and **HTCC** against A) *S. aureus* and B) *E. coli*. (*) stands for bacterial count < 50 CFU/mL.

HAp/QAm$_1$-Ag$_1$ was prepared by mixing aqueous solution of **QAm$_1$-Ag$_1$** with **HAp** and freeze-drying it. White powder-like texture was obtained on freeze drying. **HAp/QAm$_1$-Ag$_1$**was characterized by UV/Vis spectroscopy. **HAp** and **QAm$_1$-Ag$_1$** were used as references. **HAp/QAm$_1$-Ag$_1$** showed absorption of the metallic part of the composite superimposed on the absorption of **HAp** and **QAm$_1$-Ag$_1$** in the UV/Vis region (Figure 3.4). The maximum around ~260 nm corresponds to surface plasmon oscillations (SPR) of AgCl nanoparticles within the composites, which also shows the loading of the nanocomposite on **HAp**.

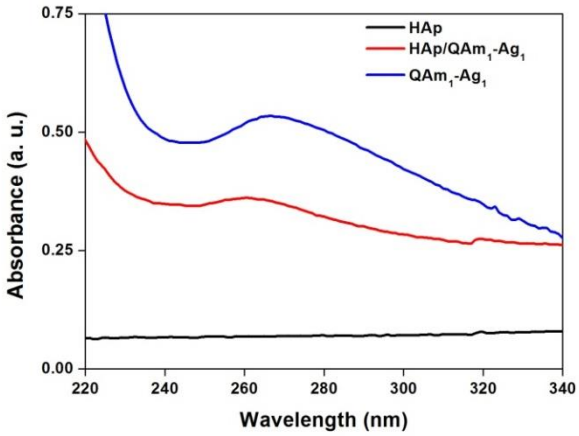

Figure 3.4: UV/Vis spectra of HAp/QAm$_1$-Ag$_1$ and HAp.

HAp/QAm$_1$-Ag$_1$ was tested for its antibacterial activity against drug resistant Gram-positive pathogen MRSA and Gram-negative pathogen *A. baumannii*. MIC value of **HAp/QAm$_1$-Ag$_1$** was 256 µg/mL against MRSA and 128 µg/mL against *A. baumannii* (Table 3.2). The loading of **QAm$_1$-Ag$_1$** in **HAp** was 5% (w/w). Hence, MIC value of 256 µg/mL against MRSA translates to 12.5 µg/mL. This value was close to the MIC of **QAm$_1$-Ag$_1$** 16 µg/mL. Similarly, against *A. baumannii*, the MIC of **HAp/QAm$_1$-Ag$_1$** was 128 µg/mL translating to 6.4 µg/mL for **QAm$_1$-Ag$_1$**, which was close to its MIC against *A. baumannii* (8 µg/mL). Hydroxyapatite (**HAp**) did not show any activity even at the highest concentration tested, i.e. 1024 µg/mL.

Both **HAp** and **HAp/QAm$_1$-Ag$_1$** were checked for their haemolytic activity (Table 3.2). HC_{50} values for both the compounds were found to be >1024 µg/mL, which proved their non-toxic nature towards human RBCs.

Table 3.2: Antibacterial efficacy and haemolytic activity of HAp and HAp/QAm$_1$-Ag$_1$

Compounds	**MIC (Minimum Inhibitory Concentration) (µg/mL)**		**HC_{50} (µg/mL)**
	MRSA	*A. baumannii*	
HAp	>1024	>1024	>1024
HAp/QAm$_1$-Ag$_1$	256	128	>1024

A susceptibility test was performed in *E. coli* and MRSA using disks formed by compacting 200 mg of **HAp/QAm$_1$-Ag$_1$**. A disk made from pure **HAp** was used as control. Inhibition of bacterial growth was not detected around the disks of **HAp**, whereas in the case of **HAp/QAm$_1$-Ag$_1$** (Figure 3.5), formation of the rings around the disks was observed. This result indicated the suppression of bacterial growth in their surroundings. The inhibition zones were mostly formed due to the diffusion of dissolved antibacterial Ag^+ ions through the agar medium. The ring around the disk in case of *E. coli* was clearer than that in case of MRSA. The diameters

of the inhibition zone were found to be 3-3.3 cm for both the bacteria. This proves the efficacy of **HAp/QAm$_1$-Ag$_1$** to kill bacteria not only upon contact, but also in its surroundings.

HC_{50} values of the materials showed that **HAp/QAm$_1$-Ag$_1$** was non-toxic to human RBCs even at 1024 µg/mL. To check whether **HAp/QAm$_1$-Ag$_1$** shows any toxicity when turned into a material containing higher amount of the sample, it was compacted into 200 mg 8 mm disks by uniaxial handpressing. RBC suspension was incubated with the disks. **HAp** was used as a control which is known to be non-toxic to human RBCs as well as other mammalian cells. The disks were incubated with human RBCs. Imaging of the cells was done to observe their morphological changes. The cells neither showed any sign of stress nor they were lysed upon exposure to **HAp/QAm$_1$-Ag$_1$** disks (Figure 3.6).

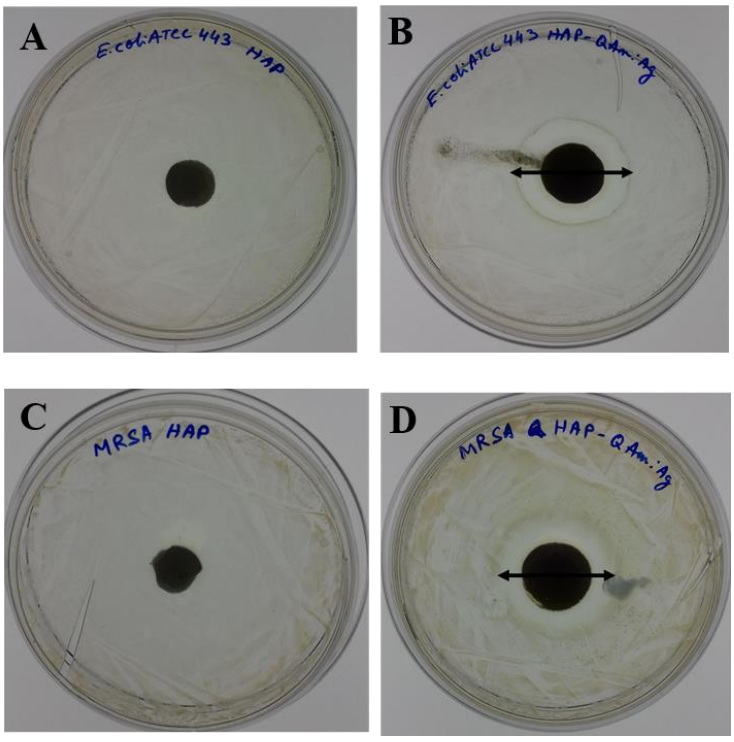

Figure 3.5: Zone of Inhibition of (A, C) **HAp** and (B, D) **HAp/QAm$_1$-Ag$_1$** against A, B) *E. coli* and C, D) MRSA.

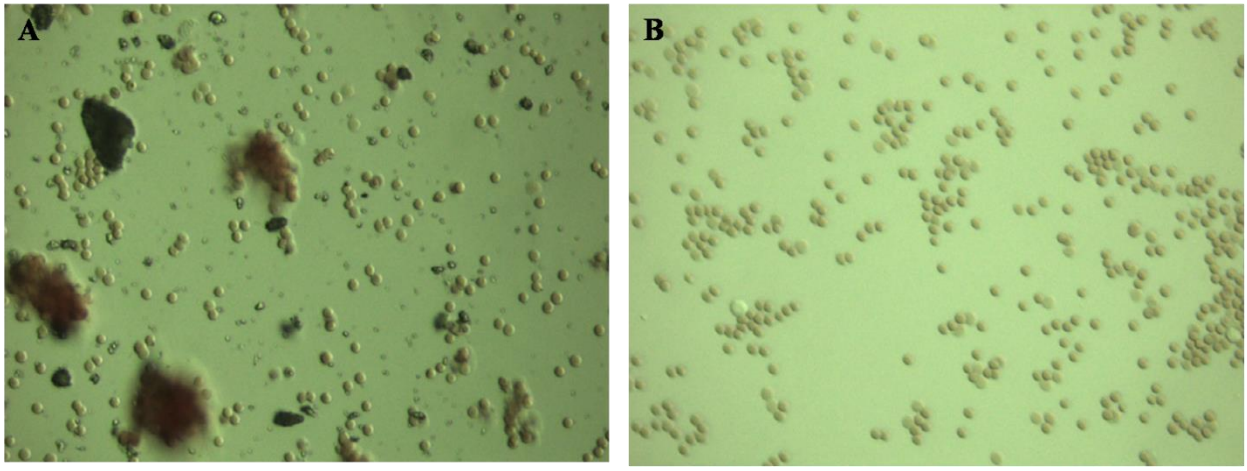

Figure 3.6: Morphology of human RBCs on disks made from A) **HAp** and B) **HAp/QAm$_1$-Ag$_1$**.

3.4 Conclusion

In conclusion, polymer-silver chloride nanocomposites were prepared from water soluble quaternary chitosan derivative HTCC and $AgNO_3$ by varying the molar ratio of quaternary amine group and silver ions. The polymer, though moderately active against Gram-positive bacteria, has very poor activity against Gram-negative pathogens. But all the nanocomposites showed very efficient activity against both Gram-positive and Gram-negative pathogens. The most active nanocomposite **QAm$_1$-Ag$_1$** had MIC values in the range of 8-32 µg/mL killing *E. coli* in 30 minutes (~5 log reduction). Hydroxyapatite, a well-known orthopedic biomaterial component was loaded with QAm$_1$-Ag$_1$ (5 % w/w). Quaternary nanocomposite loaded HAp (**HAp/QAm$_1$-Ag$_1$**) was active against Gram positive and Gram-negative pathogens. Disks made from **HAp/QAm$_1$-Ag$_1$** were shown to be non-toxic to human RBCs proving their efficacy to treat for orthopedic biomaterial related infections.

References

(1) Sanderson, P. J. *J. Hosp. Infect.* **1991,** *18*, 367.

(2) Trampuz, A.; Widmer, A. F. *Curr. Opin. Infect. Dis.* **2006,** *19*, 349.

(3) Darouiche, R. O. *N. Engl. J. Med.* **2004,** *350*, 1422.

(4) Goodman, S. B.; Yao, Z.; Keeney, M.; Yang, F. *Biomaterials* **2013,** *34*, 3174.

(5) Wong, S. Y.; Moskowitz, J. S.; Veselinovic, J.; Rosario, R. A.; Timachova, K.; Blaisse, M. R.; Fuller, R. C.; Klibanov, A. M.; Hammond, P. T. *J. Am. Chem. Soc.* **2010,** *132*, 17840.

(6) Li, Z.; Lee, D.; Sheng, X. X.; Cohen, R. E.; Rubner, M. F. *Langmuir* **2006,** *22*, 9820.

(7) Sambhy, V.; MacBride, M. M.; Peterson, B. R.; Sen, A. *J. Am. Chem. Soc.* **2006,** *128*, 9798.

(8) Min, J. H.; Choi, K. Y.; Dreaden, E. C.; Padera, R. F.; Braatz, R. D.; Spector, M.; Hammond, P. T. *ACS Nano* **2016,** *10*, 4441.

(9) Chaplin RP1, Lee AJ, Hooper RM, Clarke M. *J. Mater. Sci. Mater. Med.* **2006**, *17*,1433.

(10) Tan, H.L.; Ao; H.Y.; Ma, R.;, Lin, W. T.; Tang, T. T. *Antimicrob. Agents Chemother.* **2014** *58*, 6016.

(11) Shikinami, Y.; Okuno, M. *Biomaterials* **2001**, *22*, 3197.

(12) Yasunaga, T.; Matsusue, Y.; Furukawa, T.; Shikinami, Y.; Okuno, M.; Nakamura, T. *J. Biomed. Mater. Res.* **1999**, *47*, 412.

(13) Ashammakhi, N.; Peltoniemi, H.; Waris, E.; Suuronen, R.; Serlo, W.; Kellomaki, M. *Plast. Reconstr. Surg.* **2001**, *108*,167.

(14) Mohamed-Hashem, I.K.;, Mitchell, D.A. *Br. J. Orthodontics* **2000,** *27*, 198.

(15) Rai, M.; Yadav, A.; Gade, A. *Biotechnol. Adv.* **2009,** *27*, 76.

(16) Monteiro, D. R.; Gorup, L. F.; Takamiya, A. S.; Ruvollo, A. C.; Camargo, E. R.; Barbosa, D. B. *Int. J. Antimicrob. Agents* **2009,** *34*, 103.

(17) Feng, Q. L.; Wu, J.; Chen, G. Q.; Cui, F. Z.; Kim, T. N.; Kim, J. O. *J. Biomed. Mater. Res.* **2000,** *52*, 662.

(18) Eckhardt, S.; Brunetto, P. S.; Gagnon, J.; Priebe, M.; Giese, B.; Fromm, K. M. *Chem. Rev.* **2013,** *113*, 4708.

(19) Hachem, R. Y.; Wright, K. C.; Zermeno, A.; Bodey, G. P.; Raad, I. I. *Biomaterials* **2003,** *24*, 3619.

(20) Melaiye, A.; Sun, Z. H.; Hindi, K.; Milsted, A.; Ely, D.; Reneker, D. H.; Tessier, C. A.; Youngs, W. J. *J. Am. Chem. Soc.* **2005,** *127*, 2285.

(21) Lu, Y.; Liu, G. L.; Lee, L. P. *Nano Lett.* **2005,** *5*, 5.

(22) Dowling, D. P.; Donnelly, K.; McConnell, M. L.; Eloy, R.; Arnaud, M. P. *Thin Solid Films* **2001,** *398*, 602.

(23) Jiang, H. Q.; Manolache, S.; Wong, A. C. L.; Denes, F. S. *J. Appl. Polym. Sci.***2004,** *93*, 1411.

(24) Affinito, J.; Martin, P.; Gross, M.; Coronado, C.; Greenwell, E. *Thin Solid Films* **1995,** *270*, 43.

(25) Hoque, J.; Adhikary, U.; Yadav, V.; Samaddar, S.; Konai, M. M.; Prakash, R. G.; Paramanandham, K.; Shome, B. R.; Sanyal, K.; Haldar, J. *Mol. Pharmaceutics* **2016**, *13*, 3578.